國立陽明交通大學
NATIONAL YANG MING CHIAO TUNG UNIVERSITY

國家同步輻射研究中心

自由電子雷射
冬季課程
Winter School on Free Electron Lasers
2026
01/05~01/09

Applications of THz radiation in condensed matter physics

杜 建 明 Chien-Ming Tu

Department of Electrophysics,
National Yang Ming Chiao Tung University

2025.01.08

Outline

1. Introduction
   Pump-probe spectroscopy/Time-resolved spectroscopy

2. Terahertz emission spectroscopy

3. Intense-THz-driven nonlinear spectroscopy of condensed matters

Pump-probe spectroscopy/Time-resolved spectroscopy: Basic concept

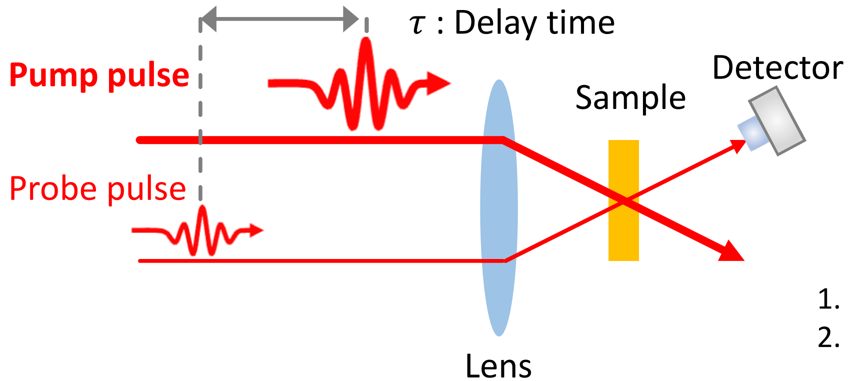

1. Wavelength
2. Polarization etc.

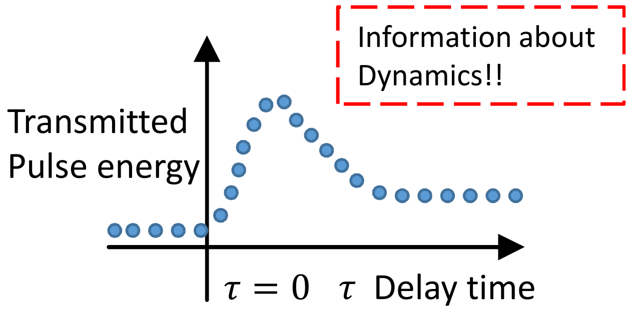

Nobel Prize Museum

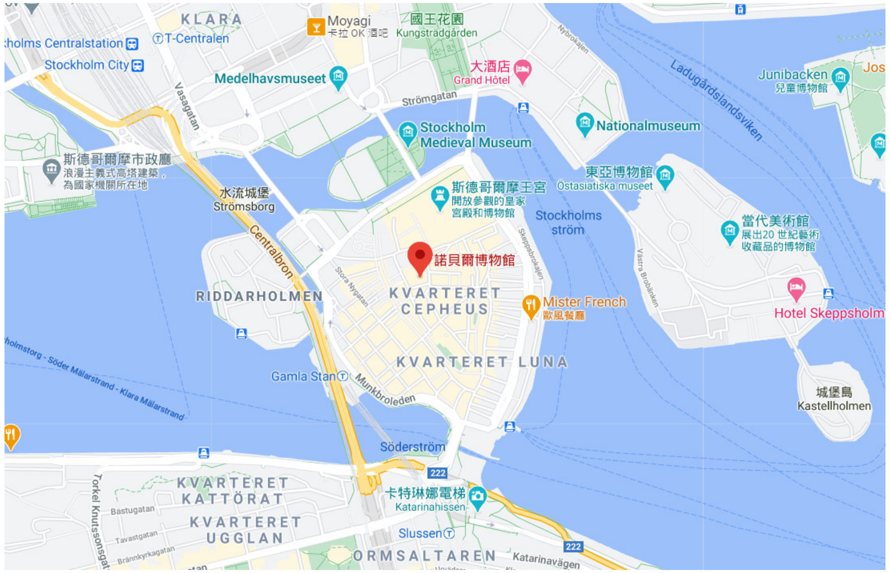

Nobel Prize Museum, Stockholm, Sweden

https://nobelprizemuseum.se/

Pump-probe spectroscopy: Basics concept

Ahmed H. Zewail
1946-2016
The Nobel Prize in Chemistry 1999

A.H. Zewail's apparatus

Femtochemistry:
the study of chemical reactions across femtoseconds.

Pump-probe spectroscopy

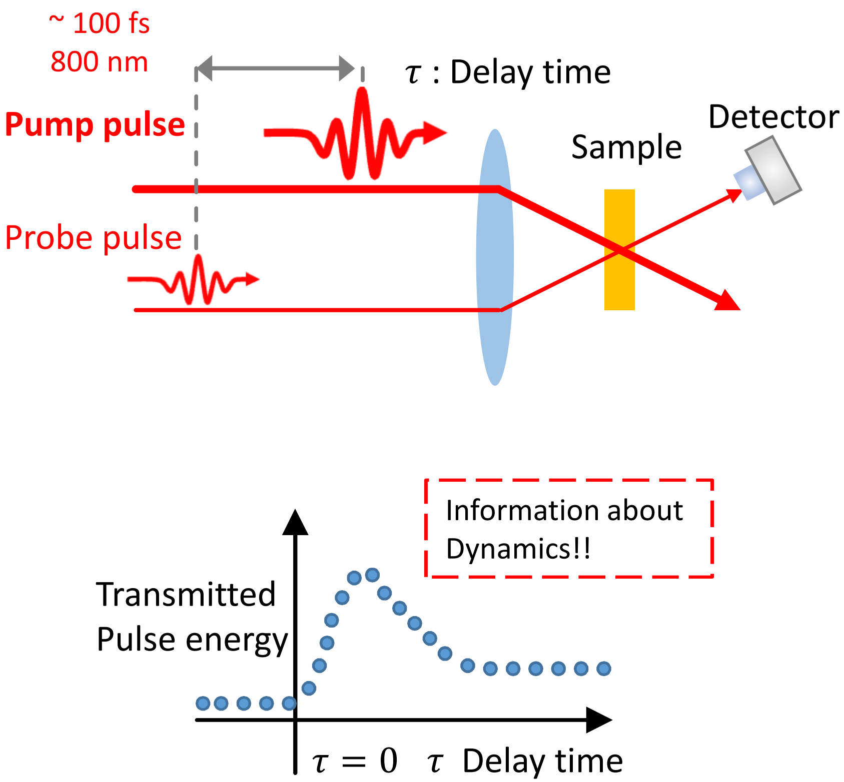

Optical pump-MIR probe on Bi_2Se_3

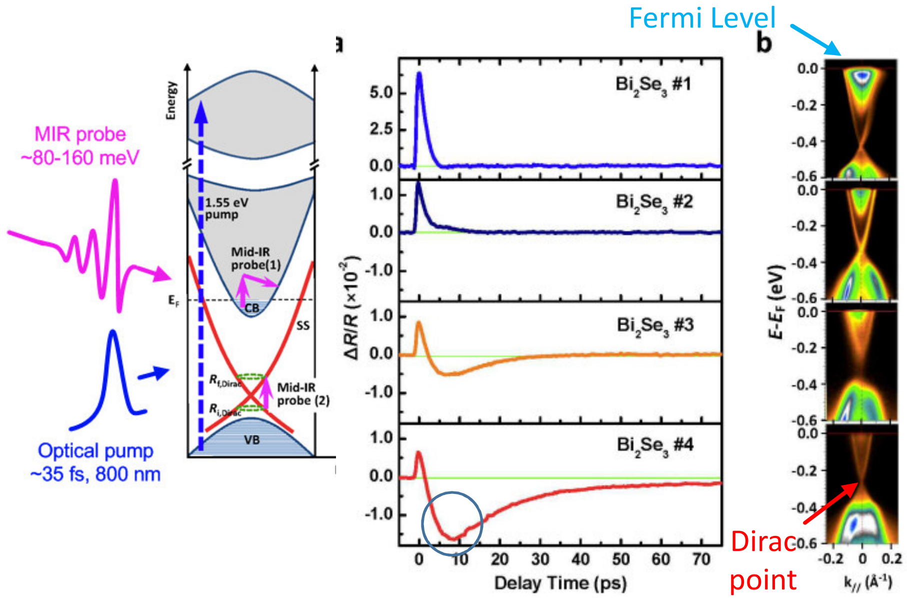

C. W. Luo, Nano Lett. **13**, 5797 (2013)

Angle-Resolved PhotoEmission Spectroscopy (ARPES)

ARPES: Static

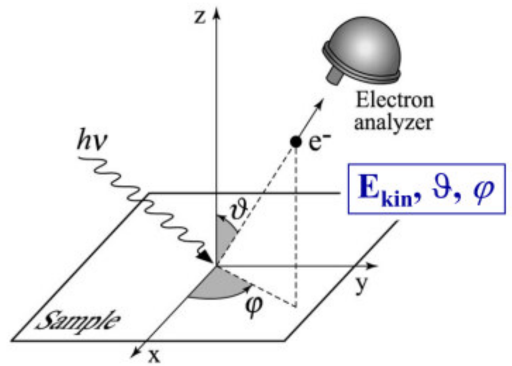

Energy Conservation

$$E_{kin} = h\nu - \phi - |E_B|$$

Momentum Conservation

$$\hbar \mathbf{k}_{\parallel} = \hbar \mathbf{K}_{\parallel} = \sqrt{2mE_{kin}} \cdot \sin\vartheta$$

Time-resolved ARPES

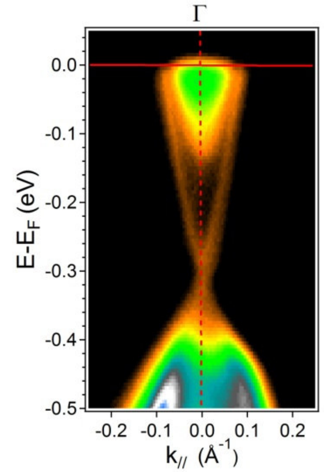

Courtesy of C.M. Cheng (NSRRC)

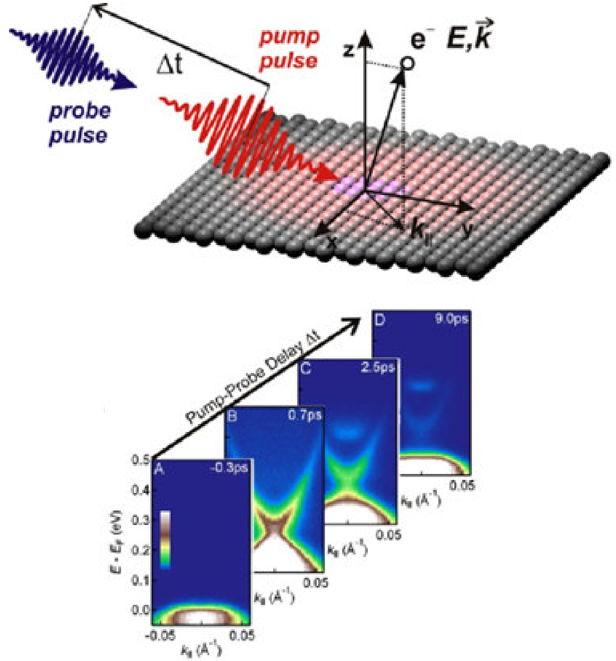

Source: Andrea Damascelli, University of British Columbia
http://qmlab.ubc.ca/ARPES/PRESENTATIONS/Talks/ARPES_Intro.pdf

Source: Fritz-Haber-Institut der Max-Planck-Gesellschaft
http://www.fhi-berlin.mpg.de/pc/PCres_methods.html

Time-Resolved-Angle-Resolved PhotoEmission Spectroscopy

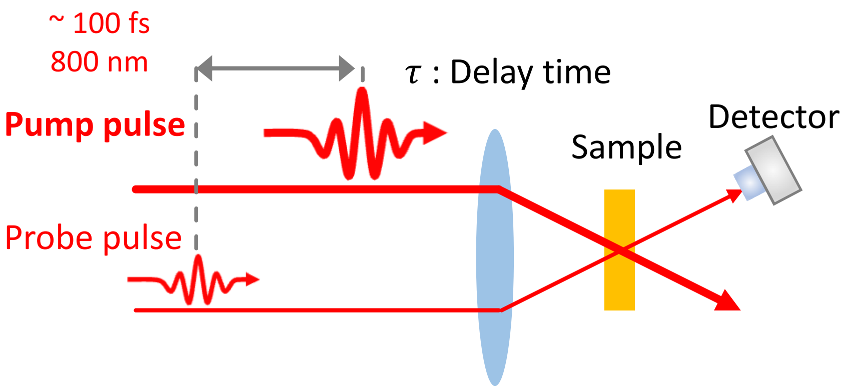

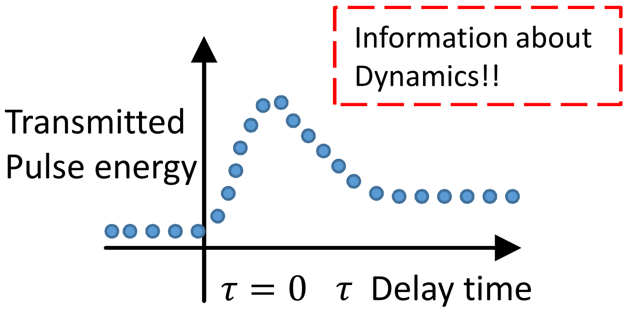

TR-ARPES

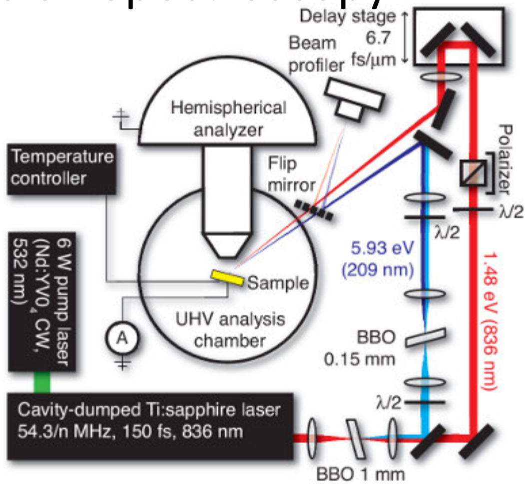

http://research.physics.berkeley.edu/lanzara/trarpes.html

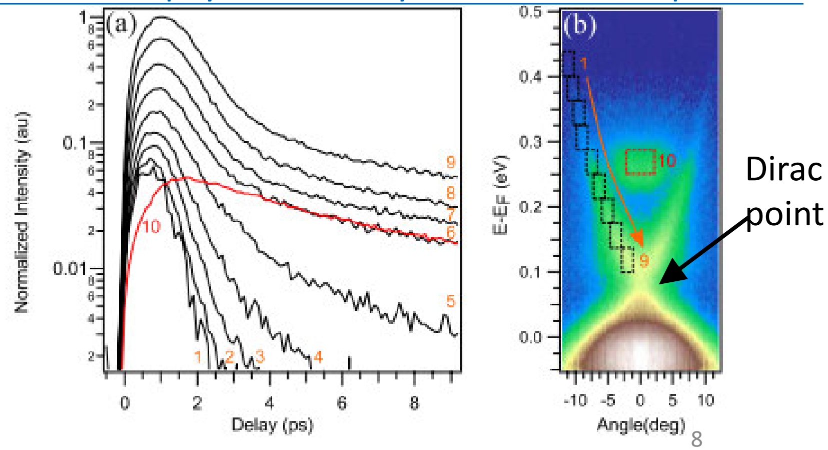

J. A. Sobota et al, PRL **108**, 117403 (2012)

Time-Resolved Spectroscopy: Free-Electron Laser (FEL)

LCSL@SLAC

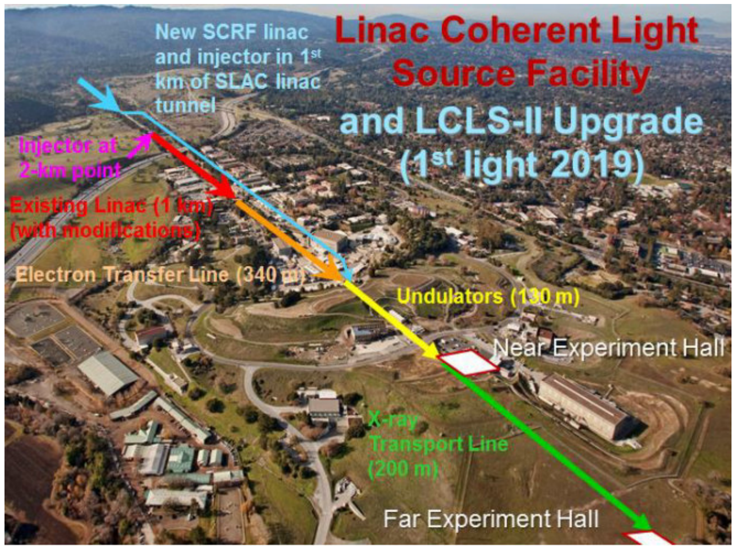

World's First Hard X-ray Free-electron Laser
~ 10s fs, E_{photon} ~ 8 keV, Δ E_{photon} ~ 1eV, 120 Hz

Time-Resolved X-Ray Diffraction: $SrTiO_3$ Soft phonon mode

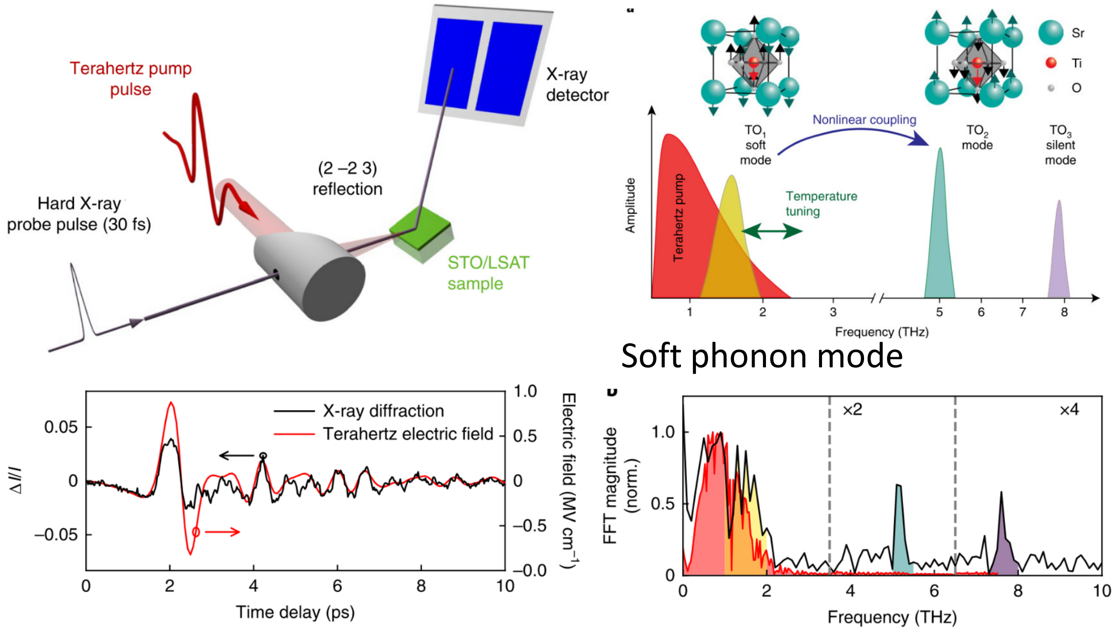

- XRD time-domain traces follow the THz E-field waveforms
- Higher frequencies of phonon modes are observed.
  → Phonon upconversion

M. Kozina *et al*, Nat. Phys. **15**, 387 (2019).

Terahertz spectrum

Terahertz spectrum

0.3 – 10 THz

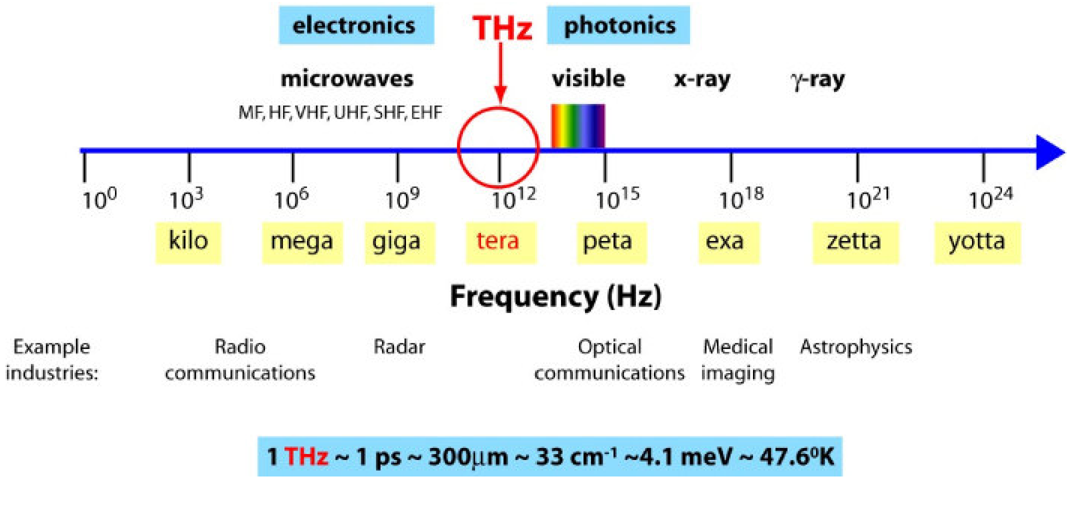

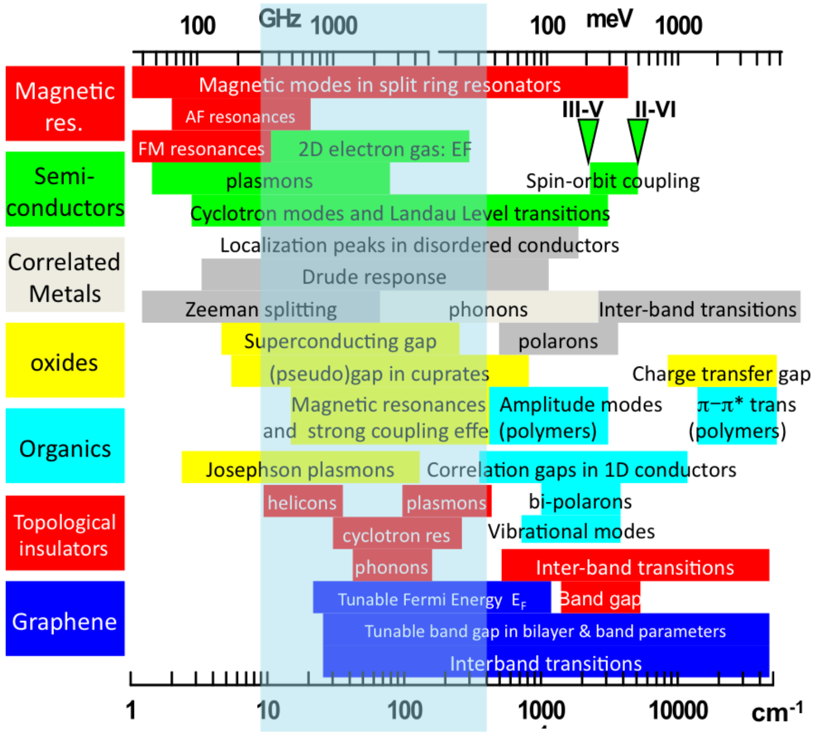

Terahertz band

D. N. Basov *et al*, "Electrodynamics of correlated electron materials", Rev. Mod. Phys. **83**, 471 (2011)

Time-Domain Spectroscopy (THz-TDS)

Time-Domain Spectroscopy (THz-TDS):
Basic experimental setup

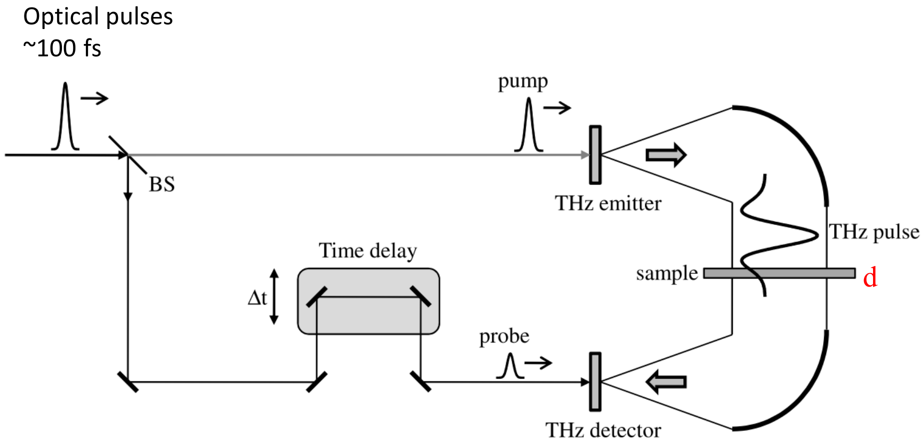

Electric amplitudes in time domain

$E_{ref}(t)$ & $E_{sam}(t)$

Fast Fourier Transform (FFT)

Complex amplitudes

$\tilde{E}_{ref}(\omega)$ & $\tilde{E}_{sam}(\omega)$

$$\frac{\tilde{E}_{sam}(\omega)}{\tilde{E}_{ref}(\omega)} = \left|\sqrt{T(\omega)}\right| \exp\left\{-i[\Delta\phi(\omega)] - \frac{\omega}{c}d\right\}$$

$$= \frac{4\tilde{n}(\omega)}{[\tilde{n}(\omega)+1]^2} \frac{\exp\left\{-i[\tilde{n}(\omega)-1]\frac{\omega}{c}d\right\}}{1-\frac{[\tilde{n}(\omega)-1]^2}{[\tilde{n}(\omega)+1]^2}\exp\left\{-i2\tilde{n}(\omega)\frac{\omega}{c}d\right\}}$$

$T(\omega)$: power transmittance
$\Delta\phi(\omega)$: intrinsic phase shift
d : sample thickness
c : speed of light in vacuum
$\tilde{n}(\omega)$: complex refractive index

$\tilde{n}(\omega) = n(\omega) + ik(\omega)$

Y. S. Lee , "Principles of terahertz science and technology"
K. Sakai, "Terahertz optoelectronics"
R. Ulbricht et al., Rev. Mod. Phys., **83**, 543 (2011)

Time-Domain Spectroscopy (THz-TDS)

Time-Domain Spectroscopy (THz-TDS):

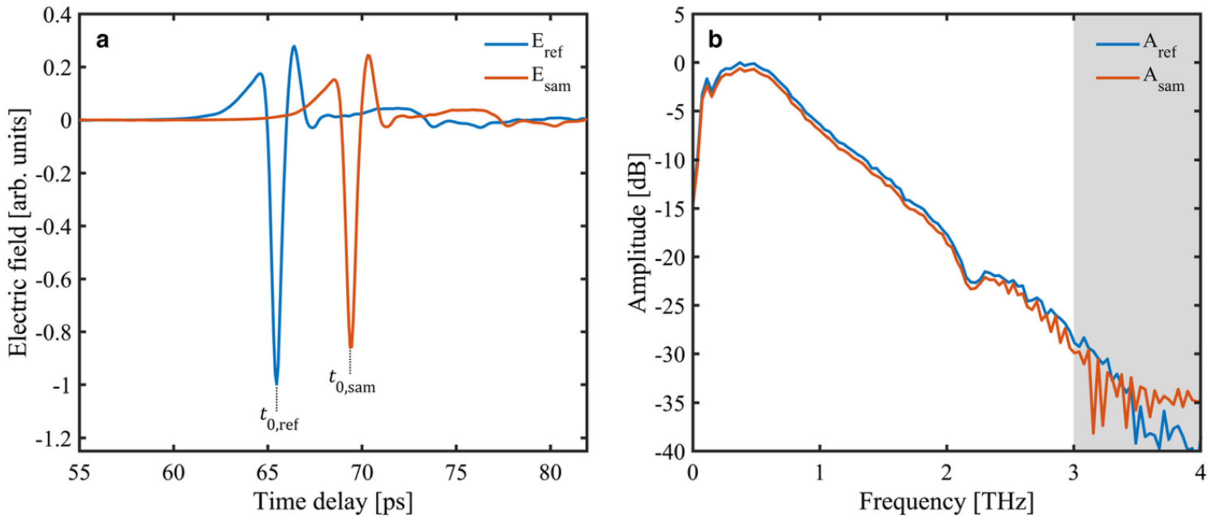

Complex refractive index
$\tilde{n}(\omega) = n(\omega) + ik(\omega)$

Dielectric function/Relative permittivity
$\tilde{\varepsilon}(\omega) = \varepsilon_1(\omega) + i\varepsilon_2(\omega) = \tilde{n}^2, \tilde{\mu} \to 1$

P. U. Jepsen, J. Infrared Milli Terahertz Waves **33**:871 (2012)

Terahertz spectrum : n-type GaAs thin film

Drude-Lorentz model

Dielectric function $\tilde{\varepsilon}(\omega) = \varepsilon_L(\omega) + i\,\frac{\sigma(\omega)}{\varepsilon_0\omega}$

Optical conductivity $\sigma(\omega) = \sigma_1(\omega) + i\sigma_2(\omega)$

Phonon contribution : $\varepsilon_L(\omega) = \varepsilon_\infty + (\varepsilon_s - \varepsilon_\infty)\frac{\omega_{TO}^2}{\omega_{TO}^2 - \omega^2 - i\omega\Gamma}$

$$\sigma(\omega) = \frac{Nq^2}{m^*}\frac{\tau}{1-\omega\tau}$$

N : electron density
τ : scattering time
m^* : effective mass

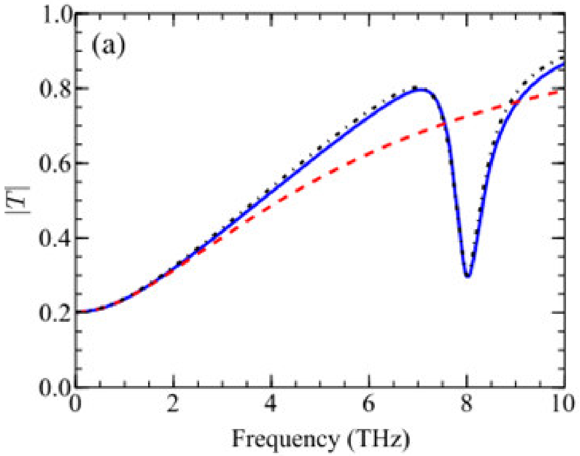

n-type GaAs, 500 nm thick
N = 1 $\times 10^{18}$ cm^{-3}
τ = 100 fs
ω_{TO}= 8.0 THz
m^*= 0.067 m_e

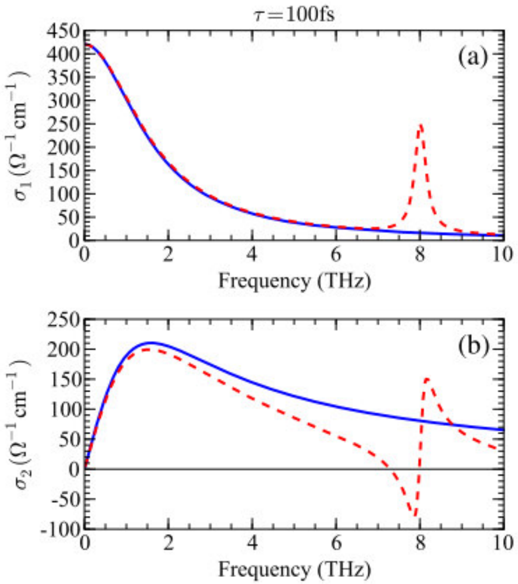

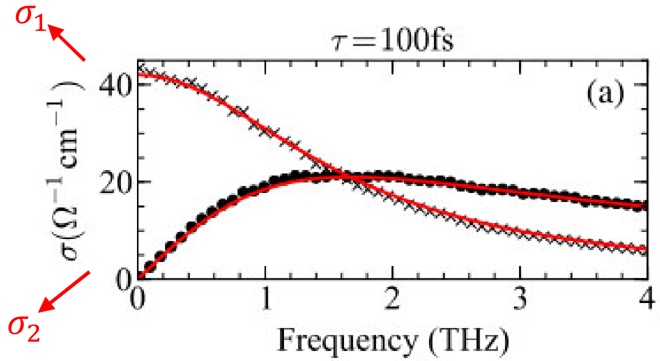

J. Lloyd-Hughes & T.I. Jeon, J. Infrared Milli Terahertz Waves **33**:871 (2012)

Terahertz emission spectroscopy

THz emission : Mechanisms

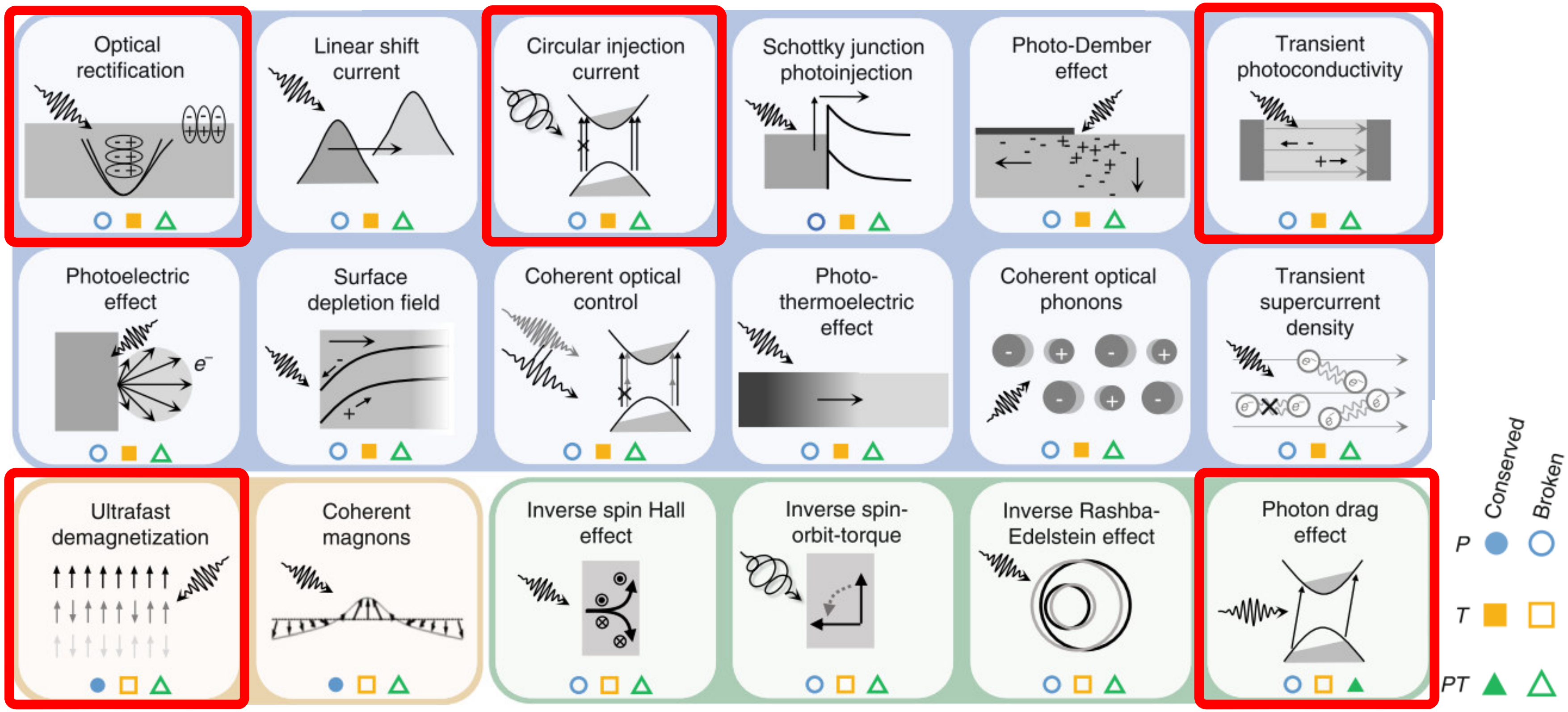

J. Pettine *et al*. Light: Science & Applications **12**, 133 (2023)

Terahertz Emission : Photocurrent

Macroscopically, the photocurrent J_λ generated by the electric field $\vec{E}$ of incident light is shown as follows

$\gamma_{\lambda\mu}$: 2nd rank pseudo-tensor for the CPGE
$\chi_{\lambda\mu\upsilon}$: 3rd rank tensor for the LPGE
$T_{\lambda\delta\mu\upsilon}$: 4th rank tensor for the PDE.
$\boldsymbol{q}_\delta$: **photon linear momentum**

$$J_\lambda = \sum_\mu \gamma_{\lambda\mu} i(\vec{E}\times\vec{E}^*)_\mu + \frac{1}{2}\sum_{\mu\upsilon}\chi_{\lambda\mu\upsilon}(E_\mu E_\upsilon^* + E_\upsilon E_\mu^*) + \sum_{\delta\mu\upsilon} T_{\lambda\delta\mu\upsilon}\boldsymbol{q}_\delta E_\mu E_\upsilon^*$$

CPGE

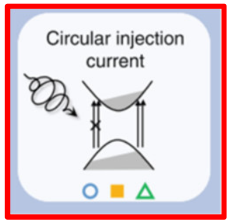

LPGE

$$J_\perp^{photon} = C\cdot\sin 2\alpha + L_1\cdot\sin 4\alpha + L_2\cdot\cos 4\alpha + D$$

PDE

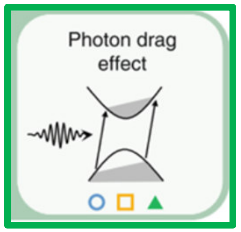

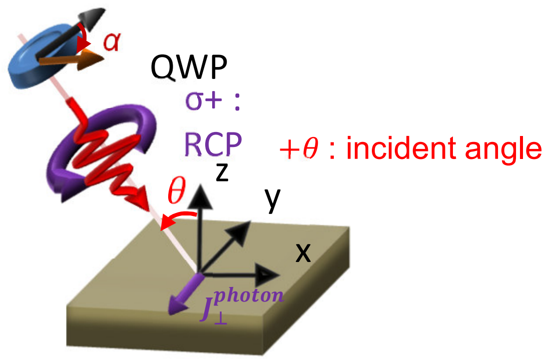

α : phase angle of QWP
C : Circular PhotoGalvanic Effect (CPGE) → Helicity-dependent
L_1 : Linaer PhotoGalvanic Effect (LPGE) → Helicity-independent
L_2 : Photon Drag Effect (PDE) → Helicity-independent
D : thermoelectric → Helicity-independent

A. Junck, Ph.D. thesis, Freie Universität Berlin, 2015.
P. Olbrich, Phys. Rev. Lett. (2014).
S. D. Ganichev and W. Prettl, J. Phys. Condens. Matter (2003).

MoS_2/WS_2 heterostructure: Interfacial current

- **MoS_2/WS_2 Heterostructure: Interfacial current**

  Type II

  A Band alignment **B**

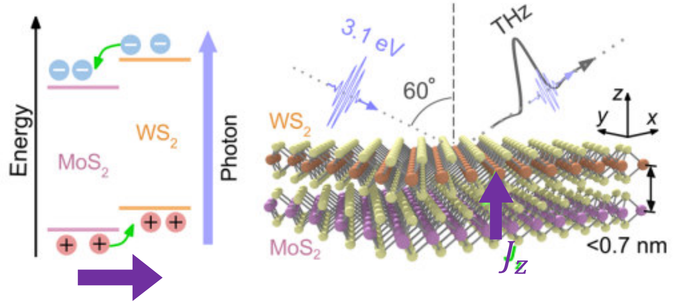

J_z : Interfacial current flows less than 0.7 nm across a van der Waals (vdW) interface.

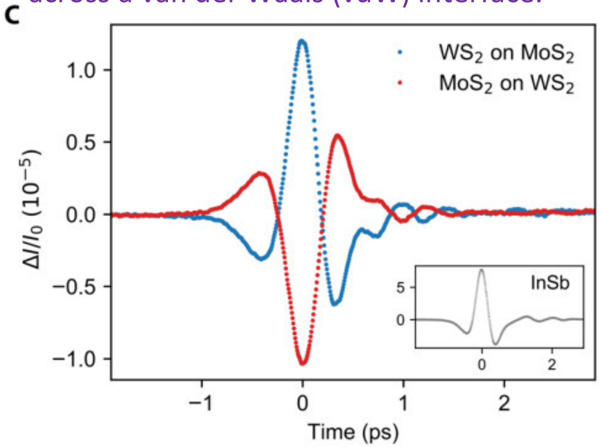

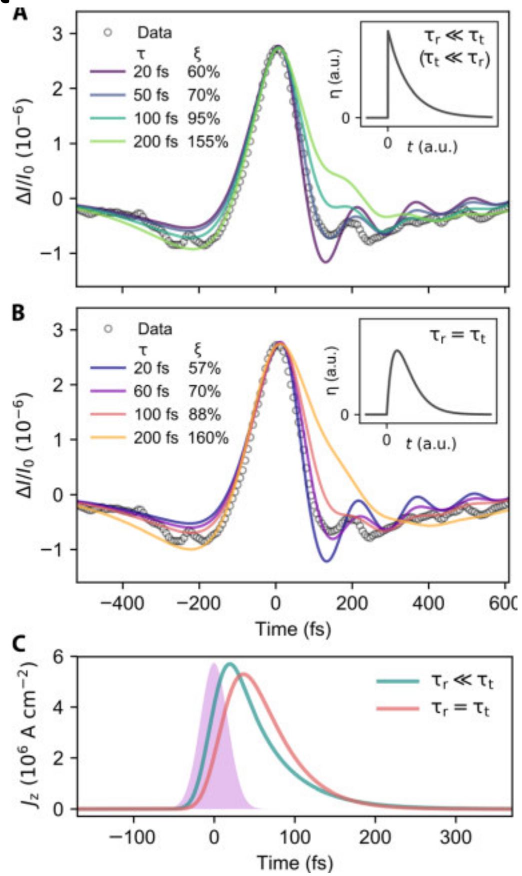

$J_z(t) = \alpha\Phi(t) * \eta(t)$

α: absorption coefficient

$\Phi(t)$:photon flux

$\eta(t)$: impulse response of *e-h* pairs

$$\eta(t) = \frac{\xi}{\tau_t - \tau_r}\left(e^{-t/\tau_t} - e^{-t/\tau_r}\right)$$

ξ: scaling factor

τ_r: *e-h* pairs relaxing time (to intermediate states)

τ_t: *e-h* pairs interlayer transferring time

$\tau = \tau_t + \tau_r$

E. Y. Ma *et al*, Sci. Adv. **5** eaau0073 (2019)

Graphene-THz Emission: Photon drag effect

Linear momentum transfer: Photon → Electron
→ transverse photocurrent

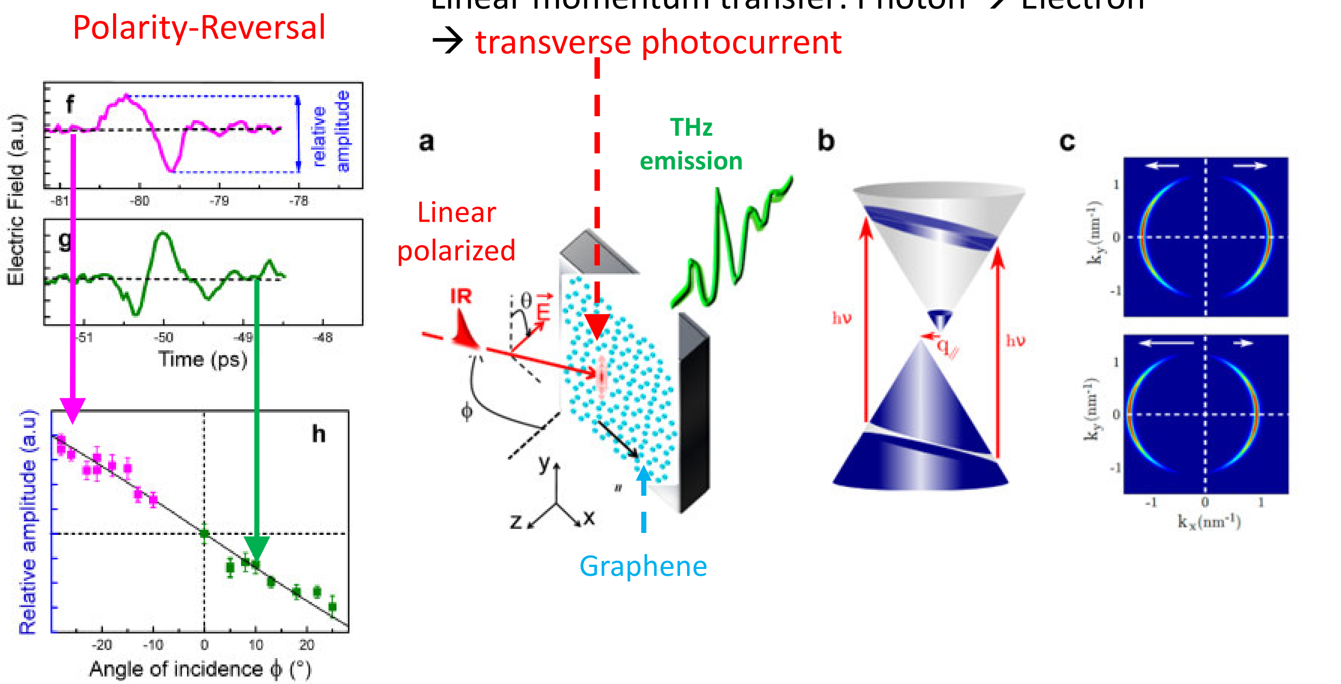

J. Maysonnave et al, Nano letters **14**, 5797 (2014).

Briefly introduction to 3D Topological insulators (TIs)

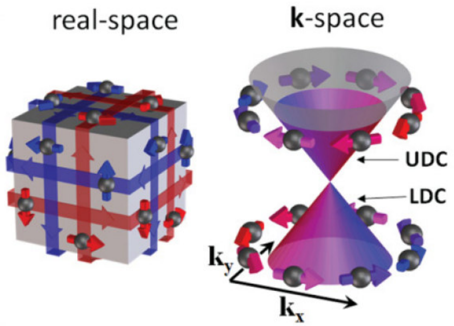

C. Jozwiak et al, PRB **84**, 165113 (2011)

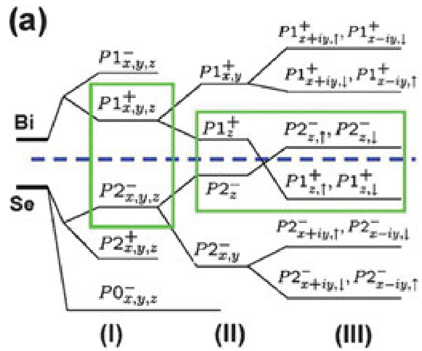

Strong spin-orbit coupling
Band inversion

Surface symmetry
$C_{3v}, \chi^{(2)} \neq 0$

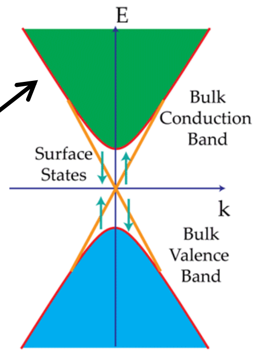

Bulk symmetry
$D_{3d}^{5}, \chi^{(2)} = 0$

Conducting surface state: time- reversal symmetry

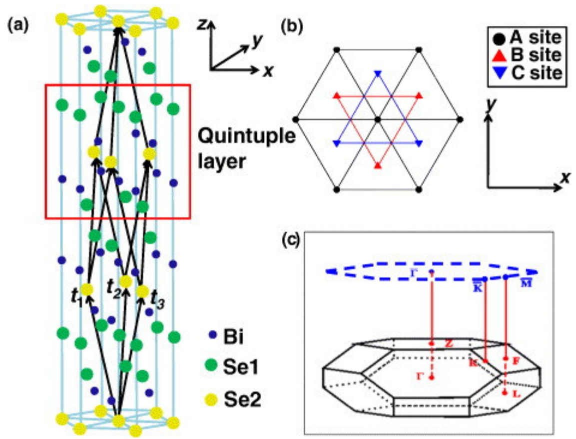

H. Zhang et al, Nature Physics **5**, 438 (2009)

TI Bi_2Se_3 : Manipulation of helicity-dependent photocurrent

Transverse $\vec{J}_{HDP}$ ⊥ Plane of incidence

λ = 795 nm, 80 fs

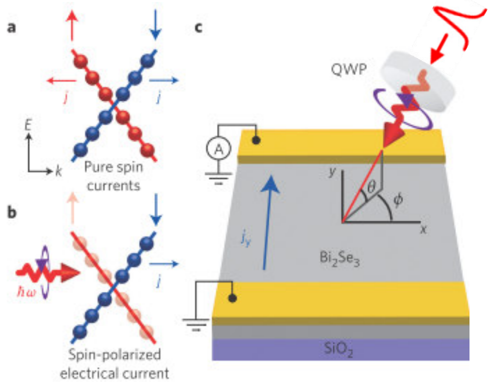

Photogalvanic Effect

Photon Drag Effect

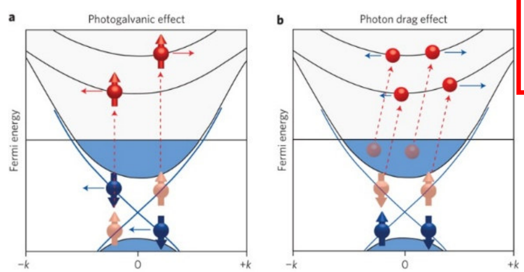

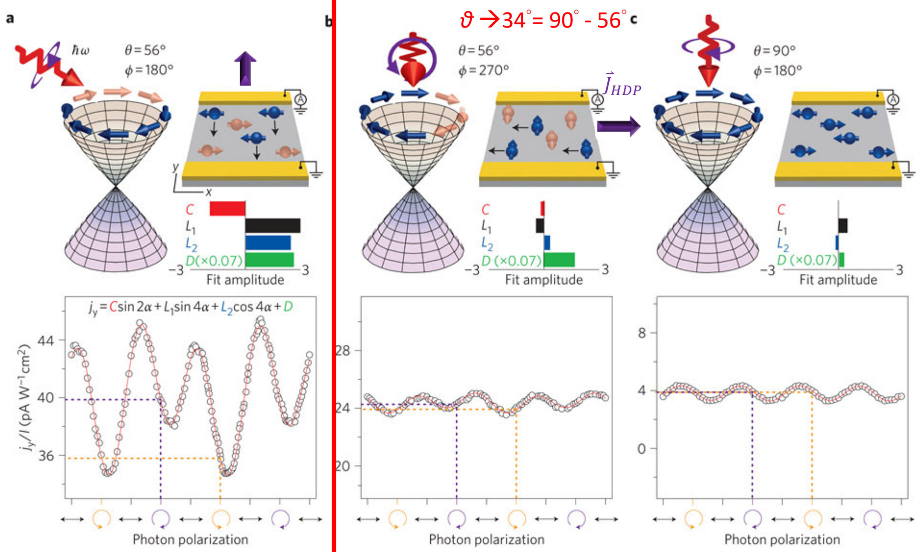

sin2α modulation

$$J_{HDP} = C * \sin 2\alpha + L_1 * \sin 4\alpha + L_2 * \cos 4\alpha + D$$

C : circular photogalvanic effect (CPGE)

L_1 : linear photogalvanic effect (LPGE)

} TSS contributions

L_2 : photon drag effect (PDE)

D : thermoelectric background

} Bulk contributions

J. McIver et al, Nature Nanotech. **7**, 96 (2012).

TI Bi_2Se_3: Ultrafast photocurrent spectroscopy

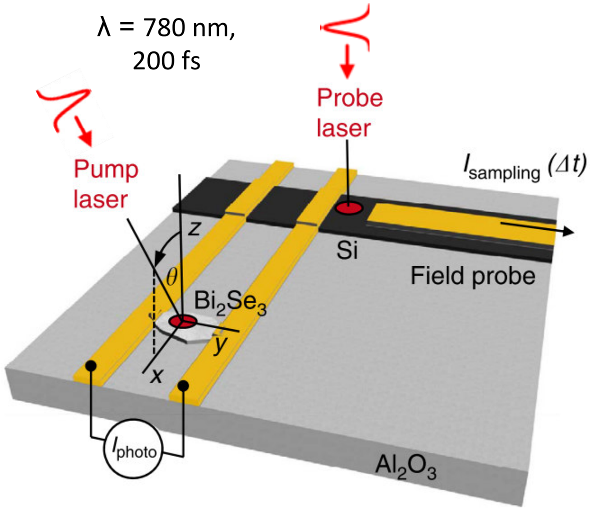

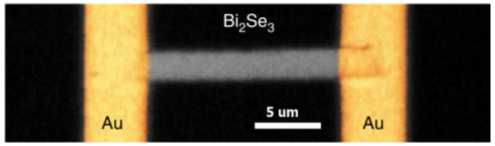

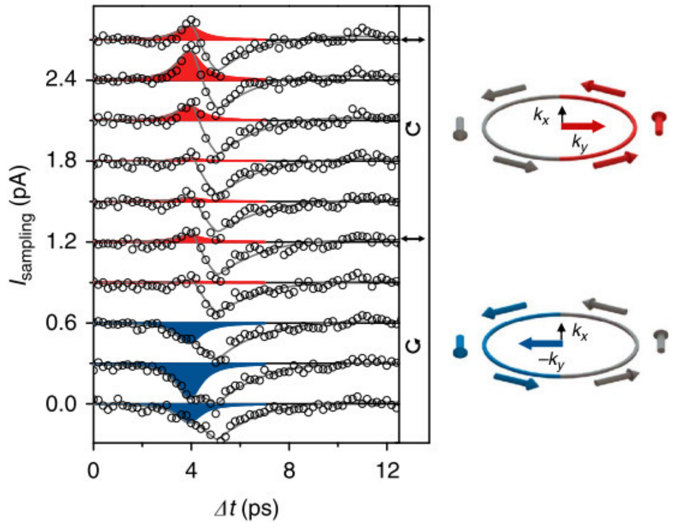

$$J_{HDP} = C * \sin 2\alpha + L_1 * \sin 4\alpha + L_2 * \cos 4\alpha + D$$

Ultrafast photocurrent @Δt = 4 ps

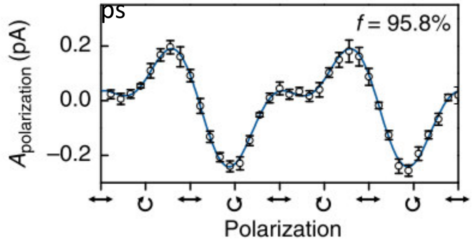

sin2α modulation

C. Kastl et al, Nature Comms. **6**, 6617 (2015).

MBE-growth TI Sb_2Te_3 thin film

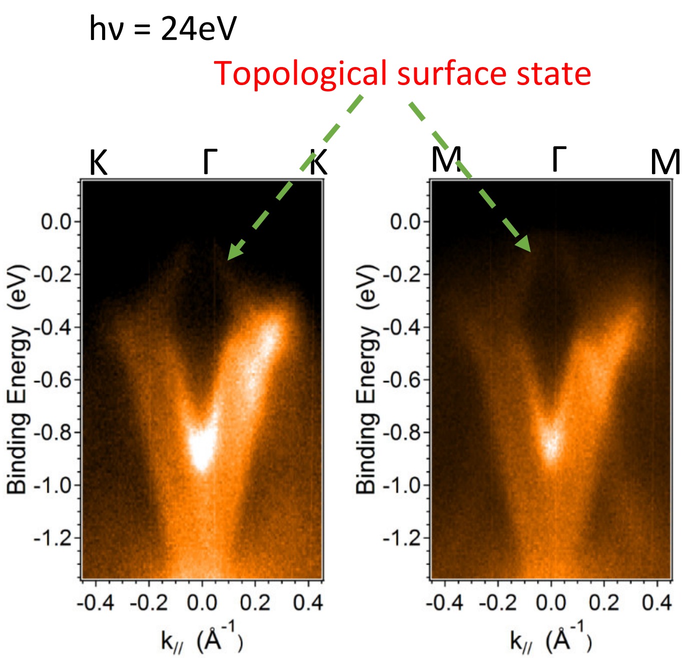

Prof. J. C. A. Huang (NCKU)

C.M. Cheng (NSRRC)

p-type Sb_2Te_3 thin film

500 um Al_2O_3

40 nm Sb_2Te_3

10 nm Se-capping

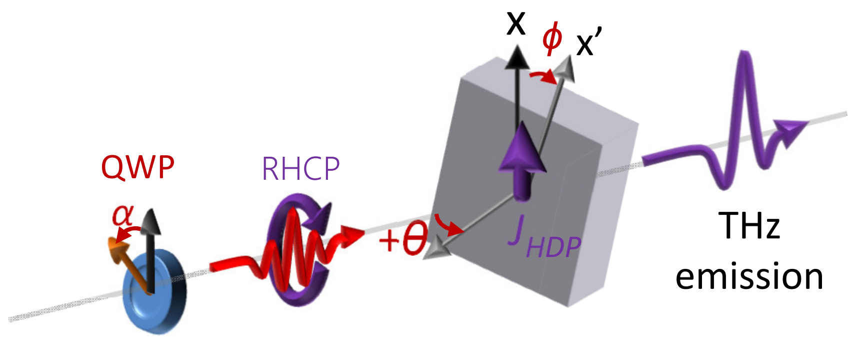

ϕ: crystal orientation angle

θ: sample tilted angle

α: phase angle of QWP

TI Sb_2Te_3 : Polarization control of helicity-dependent THz radiation@$\varphi = 0^\circ$

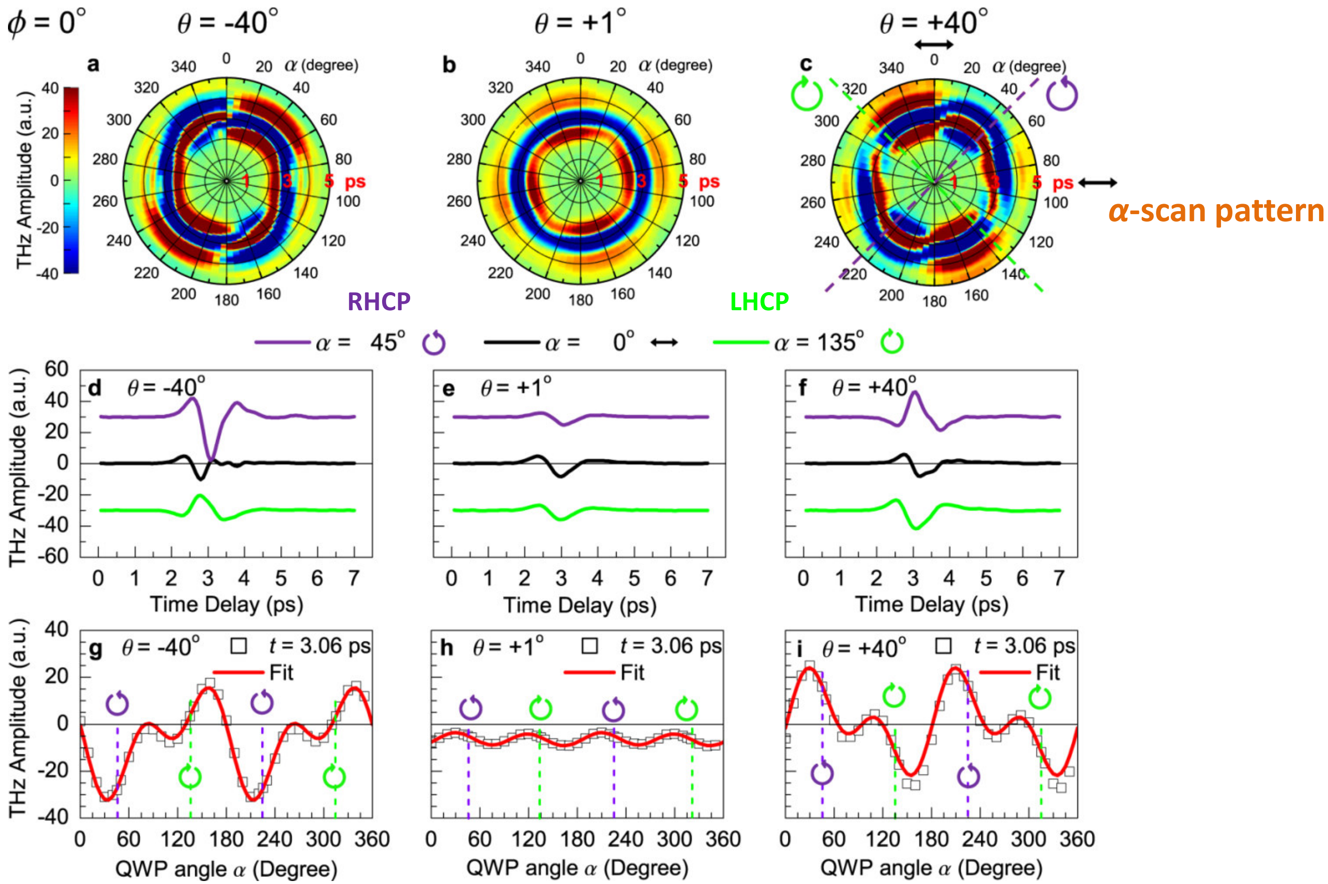

C. M. Tu *et al*, PRB **96**, 195407 (2017).

TI Sb_2Te_3: THz Radiation Time-Domain analysis @ $\varphi = 0^\circ$

$$E_{HDP}(\alpha,t) \propto C'(t) * \sin 2\alpha + L'_1(t) * \sin 4\alpha + L'_2(t) * \cos 4\alpha + O(t)$$

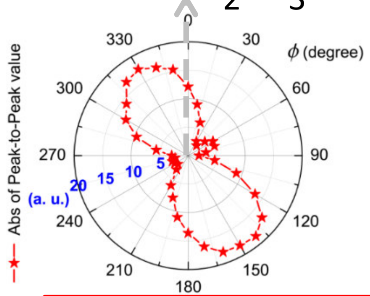

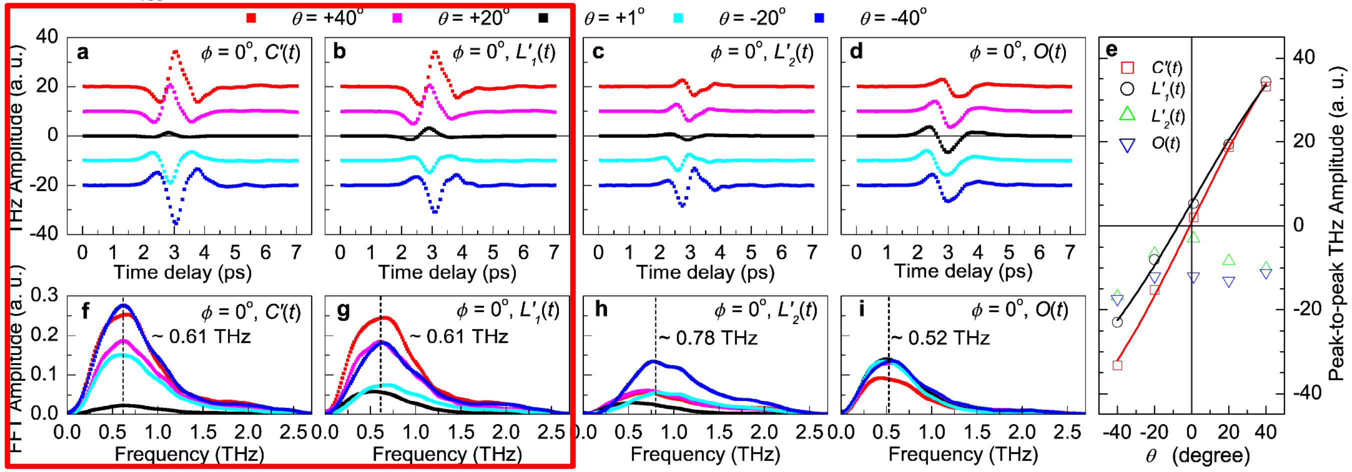

CPGE & LPGE show similar waveforms & spectra!

C. M. Tu *et al*, PRB **96**, 195407 (2017).

Sb_2Te_3: circularly-polarized time-resolved ARPES

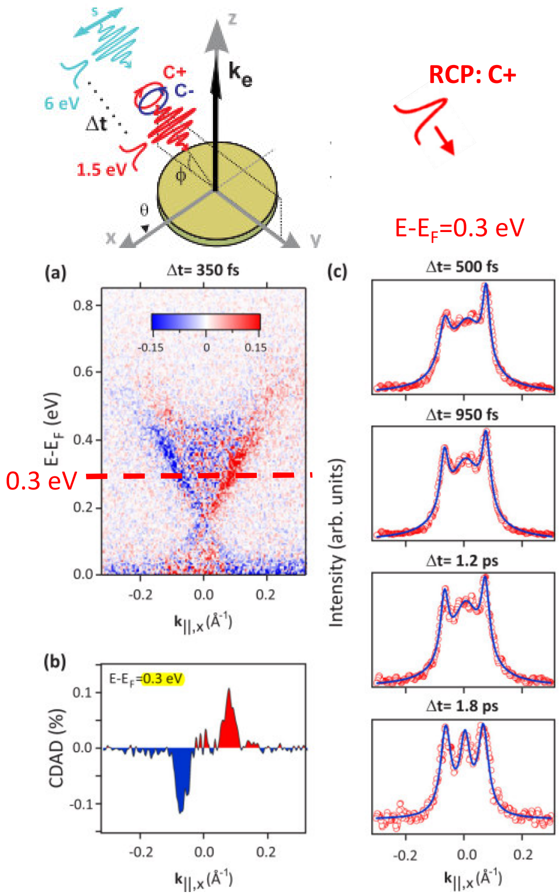

p-type Sb_2Te_3 single crystal, room temp

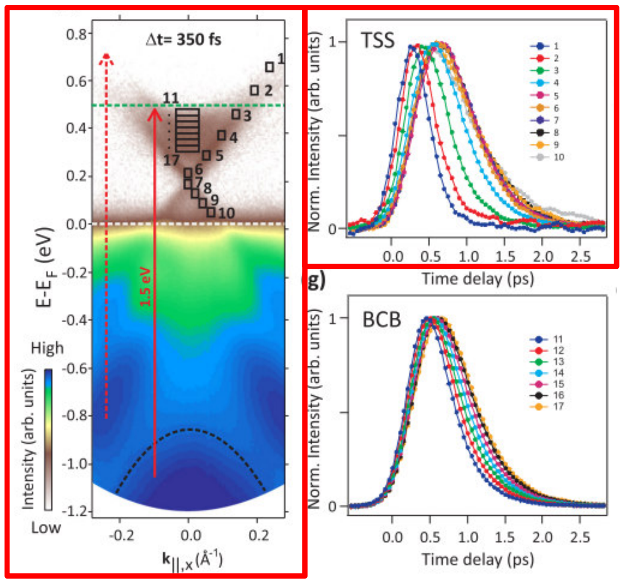

J. Sanchez-Barriga, PRB **93**, 155426 (2016).

Circularly-polarized time-resolved ARPES: THz spectra estimation

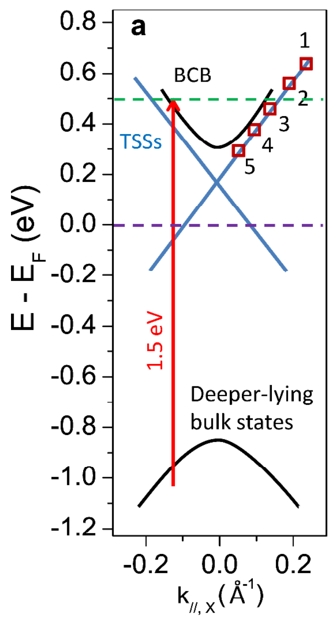

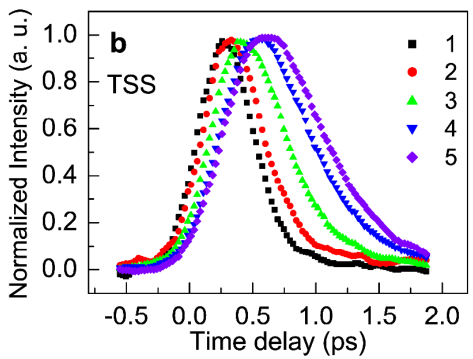

$$J = env,\ E_{THz} \propto \frac{dJ}{dt} = e\frac{dn}{dt}v$$

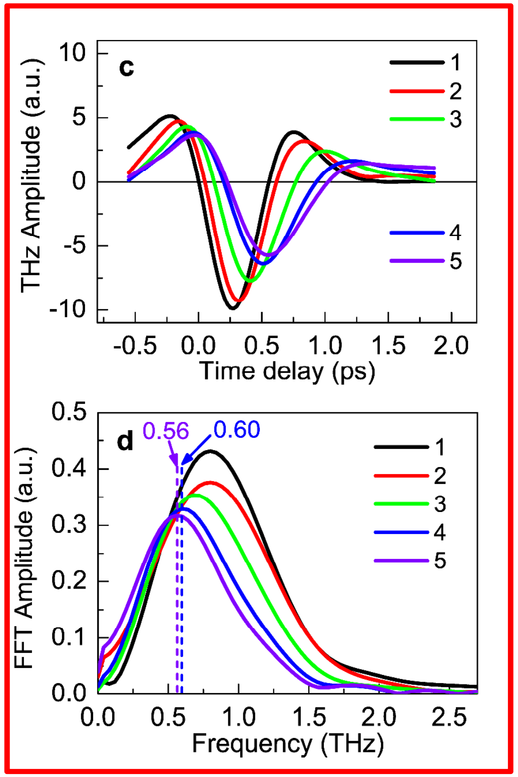

1. Re-digitalized figures: estimate the contributions of THz emission from different windows on TSS.
2. Far-field diffraction.

C. M. Tu *et al*, PRB **96**, 195407 (2017).

TIs Spin-polarized photocurrents

Helicity-dependent Time-Resolved Kerr-Rotation

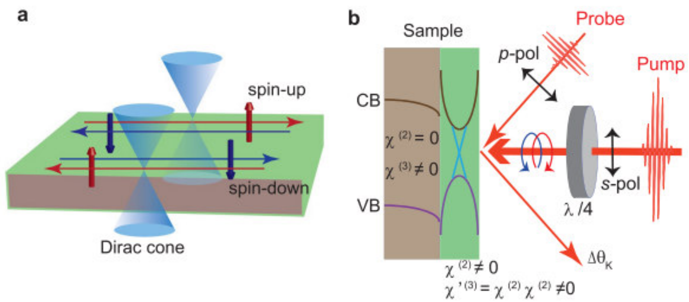

$$\Delta\theta_K = \frac{\chi}{n}\vec{M}\cdot\vec{k}$$

- $\Delta\theta_K$: Kerr-rotation signal, polarization-variation of optical pulses
- $\vec{M}$: Transient magnetization
- $\vec{k}$: wave vector of linear-polarized optical pulses
- χ: magneto-optical susceptibility
- n: refractive index of materials

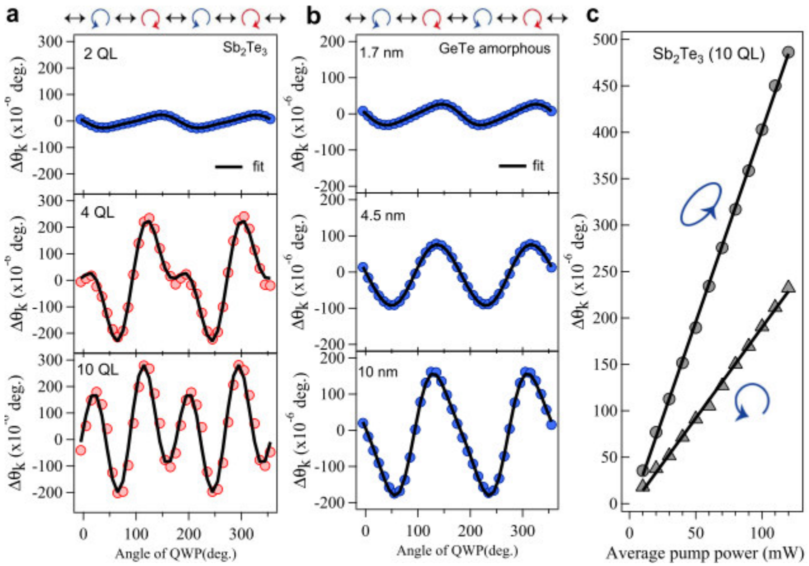

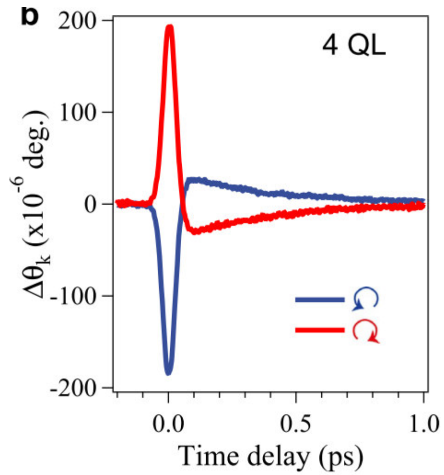

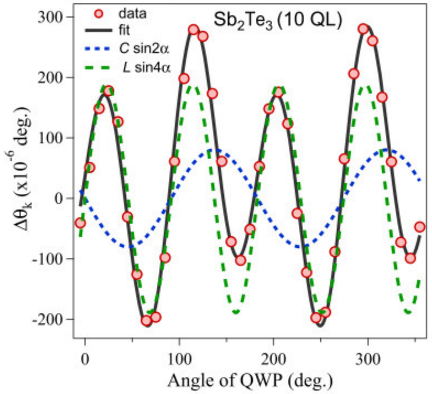

$$\Delta\theta_K = \frac{32\pi^2 I_{pump}}{c|1+n|^2}(C\sin 2\alpha + L\sin 4\alpha)$$

R. Mondal et al, Sci. Rep. **8**, 3908 (2018).

Circular PhotoGalvanic Effect : WSe_2

2DEG with Rashba spin splitting

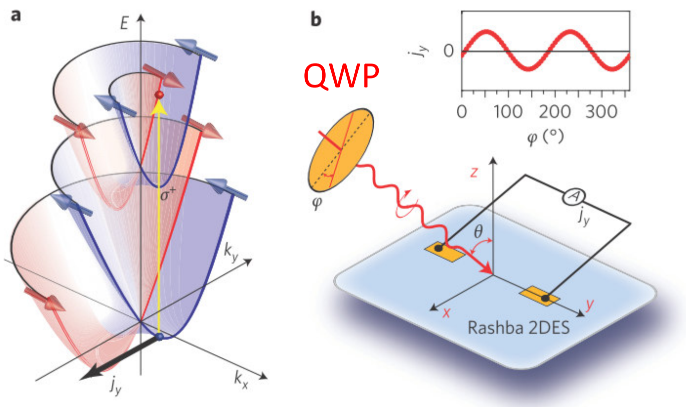

$$J_y = C\sin 2\alpha + L\sin 4\alpha + A$$

Transverse CPGE $J_{\mathrm{CPGE}} = C\sin 2\alpha$

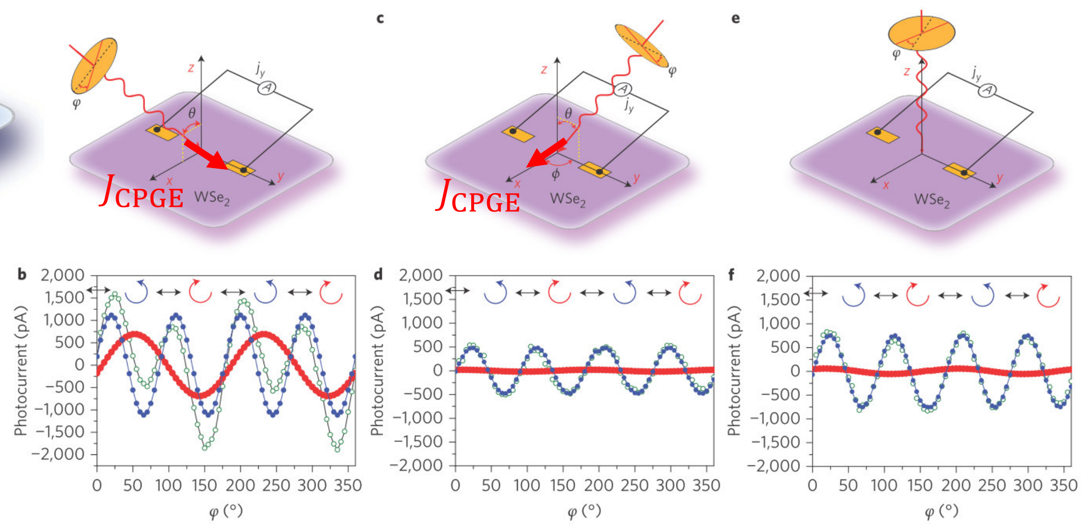

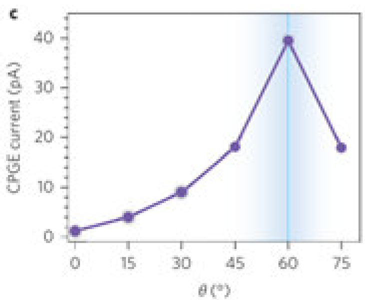

H. Yuan *et al*, Nature Nanotech. **9**, 851 (2014).

Rashba-type polar semiconductor BiTeBr

Rashba-type polar semiconductor BiTeBr

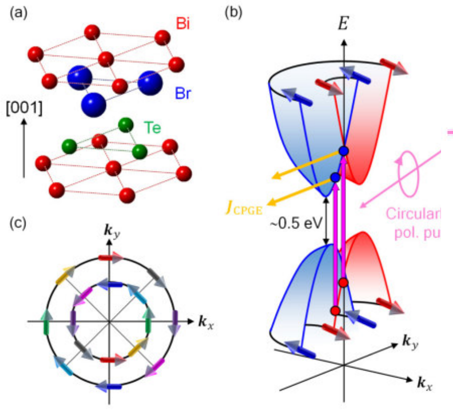

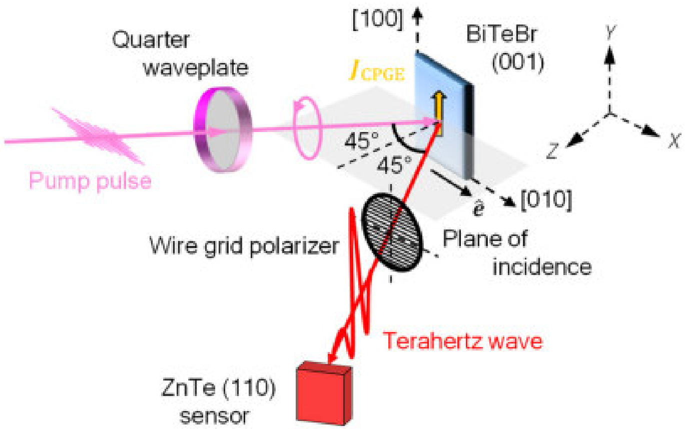

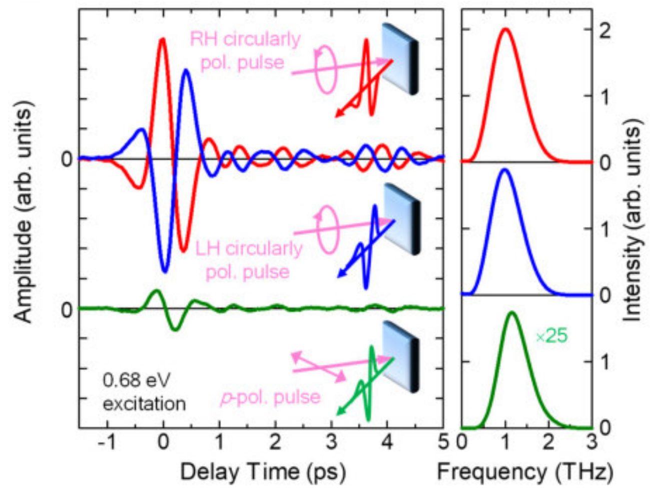

$$J_{\rm CPGE} = C\sin 2\alpha \propto \gamma \sigma_{\pm} E^2\, \hat{\boldsymbol{e}}$$

γ: second-rank tensor introduced by the Rashba Dresselhaus spin-orbit interaction

$\sigma_{\pm}(=\pm 1)$: the helicity of light

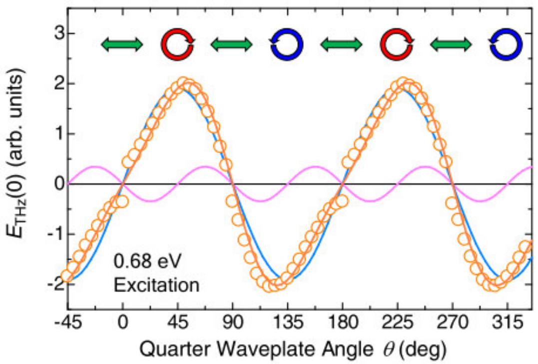

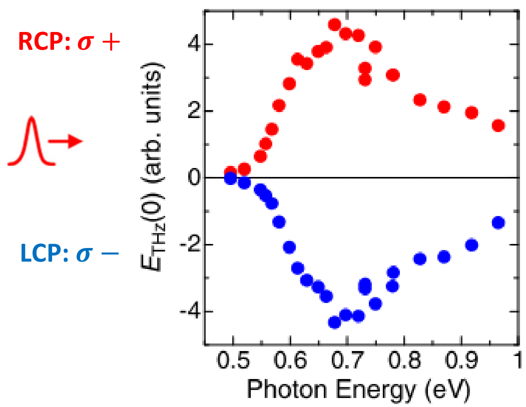

Y. Kinoshita *et al*, Phys. Rev. B. **97**, 161104 (2018).

Introduction : Classifications of Topological Materials

Topological insulator (TI)
2D conducting topological surface states (TSSs)

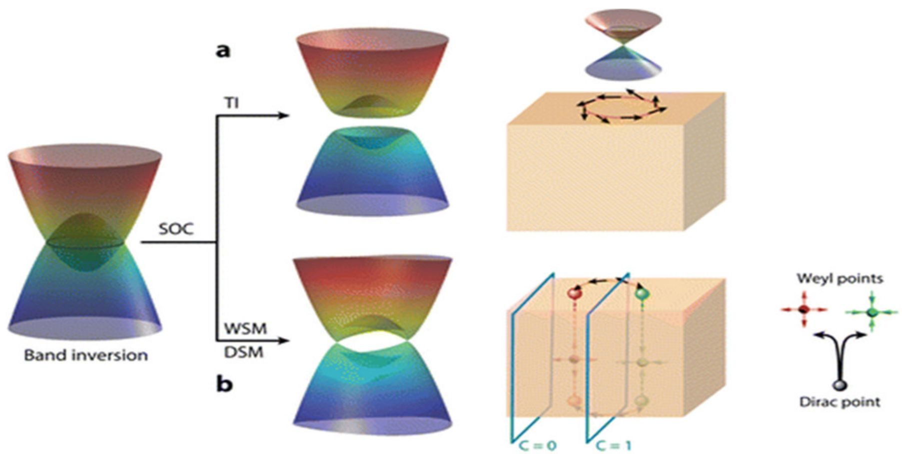

Dirac Semimetal (DSM)
Weyl Semimetal (WSM)
→ 3D analog of graphene

B. Yan and C. Felser, Annu. Rev. Condens. Matter Phys. **8** 337 (2017)

DSM → WSM
Inversion Symmetry Breaking or
Time-Reversal Symmetry Breaking

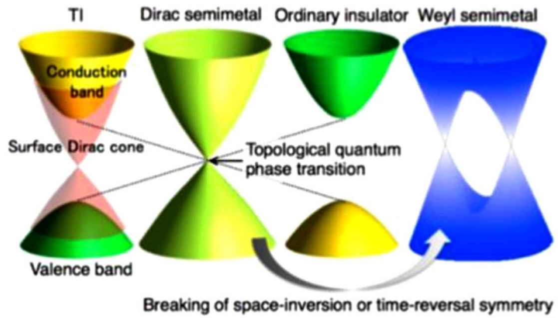

M. Kanagaraj et al, Reviews in Physics **8** (2022) 100072

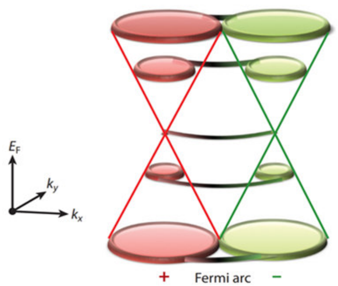

WSMs hosts Fermi arcs on the Fermi surface of the surface band structure.

Topological materials: Helicity-dependent THz emission

Topological Insulator Sb_2Te_3

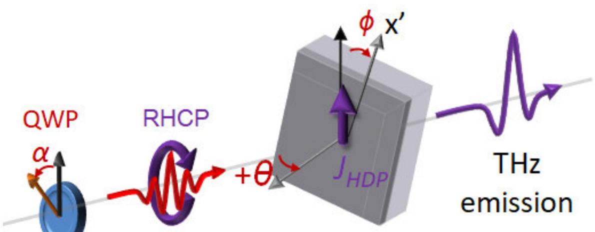

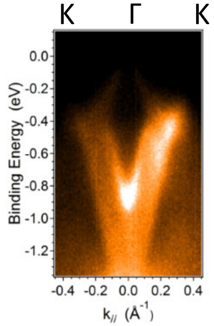

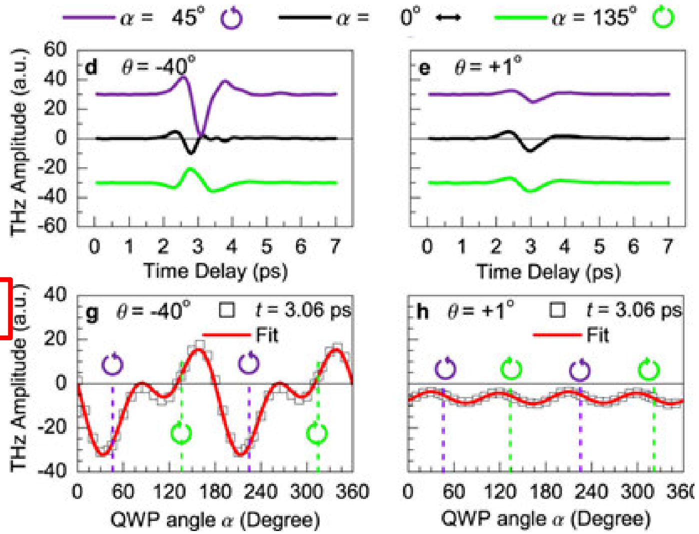

sin2α

C. M. Tu *et al*, PRB **96**, 195407 (2017).

Weyl Semimetal TaAs

Transverse CPGE

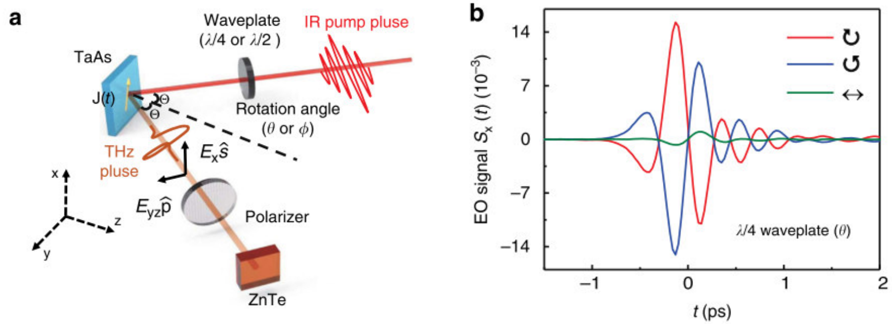

Y. Gao, *et al*, Nat. Comms. **11**, 720 (2020).

Weyl Semimetal CoSi/RhSi

CoSi

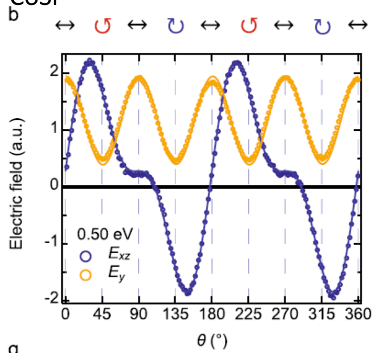

RhSi

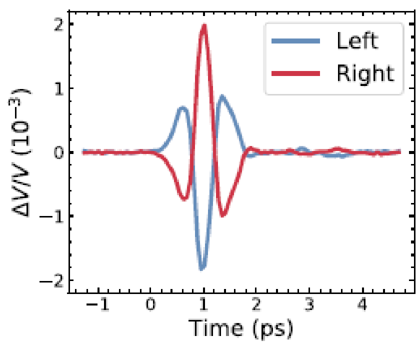

Z. Ni *et al*. Nat. Comms.,**12**, 154 (2021) R. Rees *et.al*, Sci. Adv., **6**, eaba0509 (2020).

Light-induced topological phase transition: $ZrTe_5$-Dirac semimetal-Weyl semimetal

$ZrTe_5$-Light-induced DSM-WSM (Zirconium pentatelluride: 五碲化鋯)

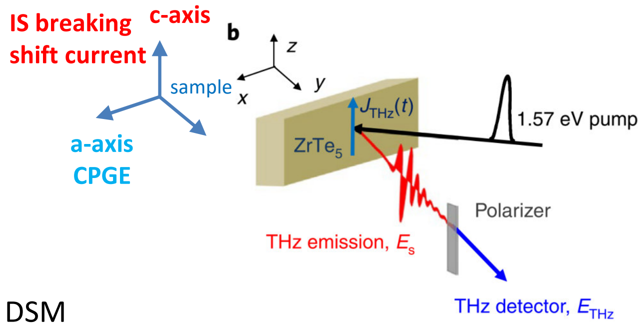

DSM
centrosymmetry

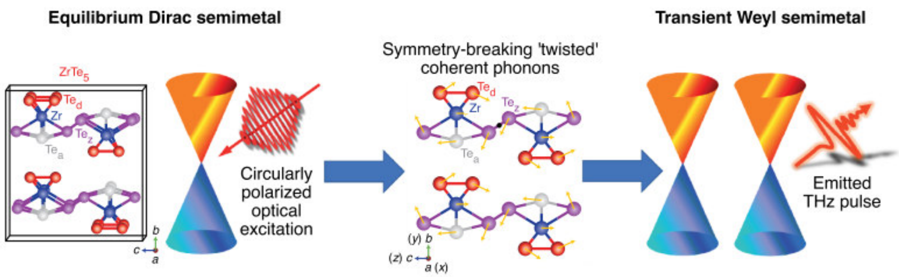

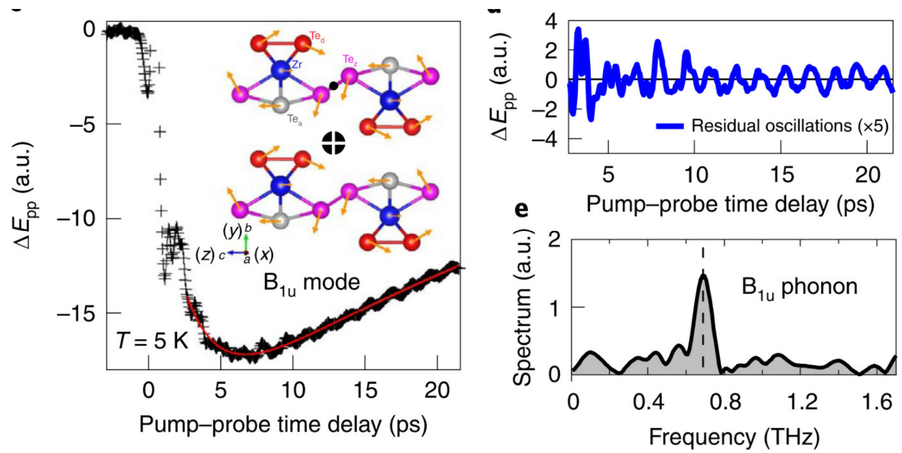

WSM
Broken Inversion Symmetry (IS)
Broken Time-Reversal Symmetry (TRS)

L. Luo et al,. Nature Mat. **20**, 329 (2021)

Light-induced topological phase transition: $ZrTe_5$-Dirac semimetal-Weyl semimetal

$ZrTe_5$-Light-induced DSM-WSM (Zirconium pentatelluride: 五碲化鋯)

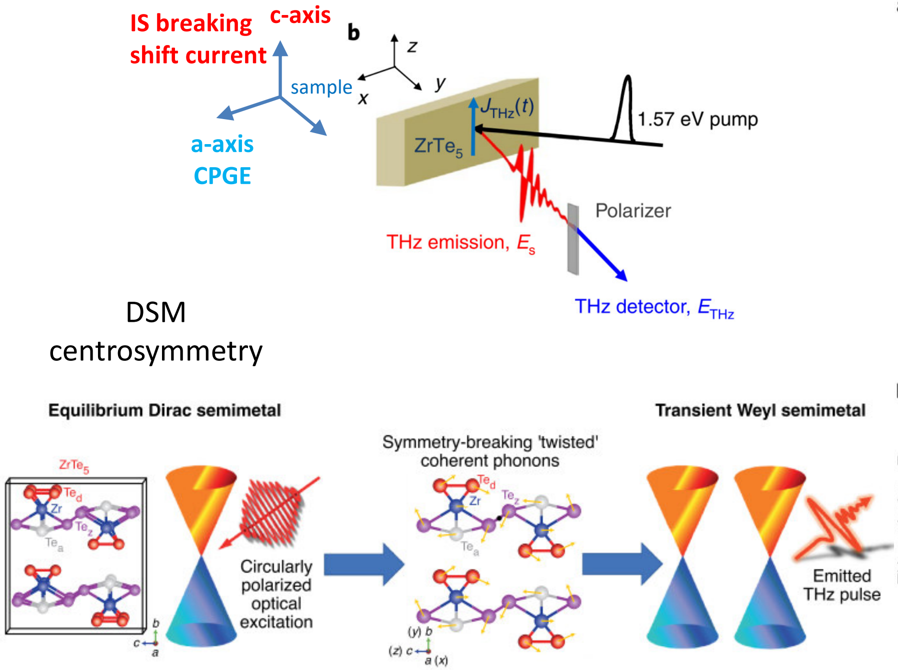

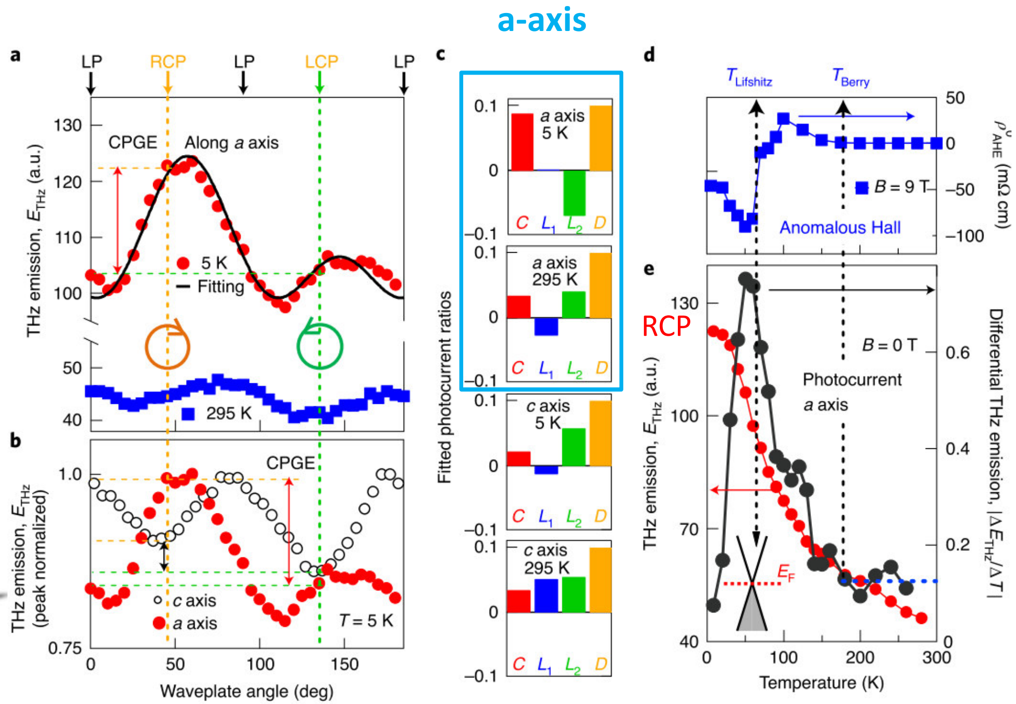

WSM

Broken Inversion Symmetry (IS)

Broken Time-Reversal Symmetry (TRS)

L. Luo et al,. Nature Mat. **20**, 329 (2021)

Intense-THz-driven Nonlinear Spectroscopy

of

Condensed Matters

Nobel Prize in Physics 2018: **Chirped Pulse Amplification**

Arthur Ashkin **Gérard Mourou** **Donna Strickland**

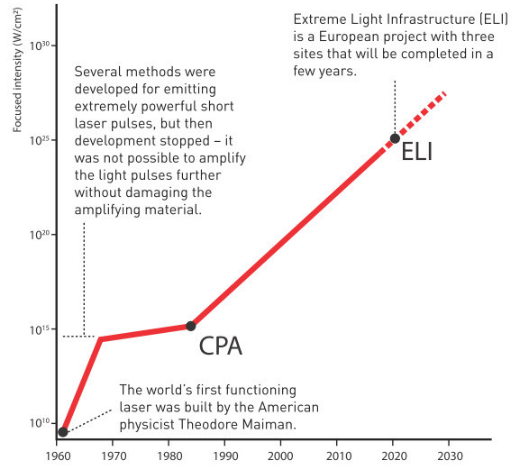

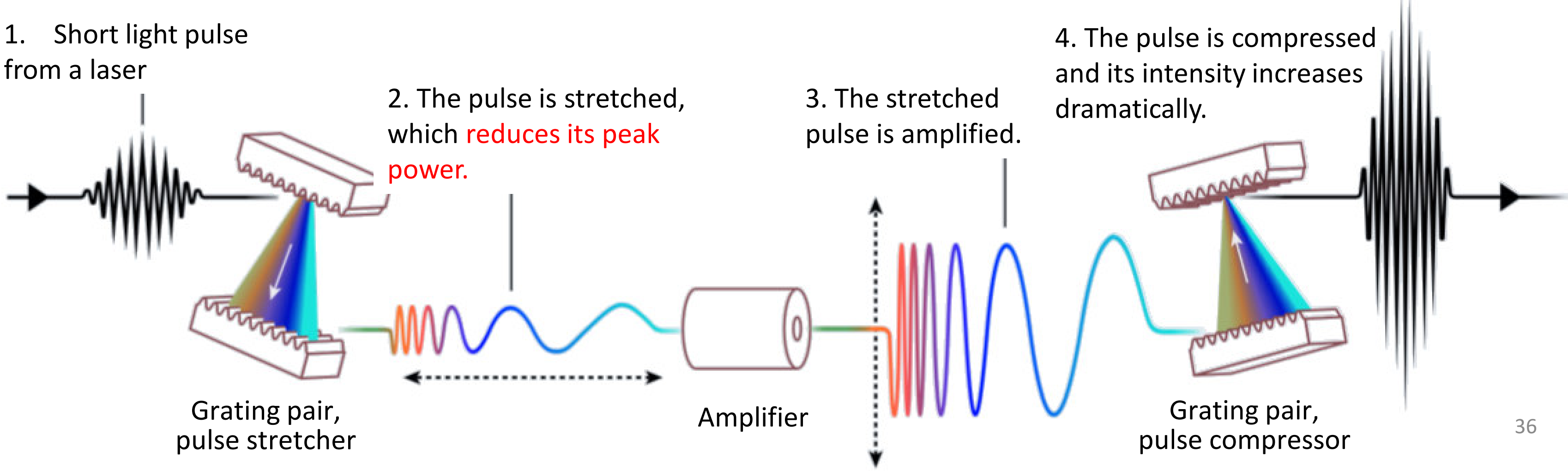

Table-top, Laser-based, Intense THz source: Tilted Pulse Front in $LiNbO_3$

Nonlinear optical materials for THz generation

Material	d_{eff} [pm/V]	n_g @ 800 nm (1.55 μm)	n_{THz}	α_{THz} [cm^{-1}]	FOM for L = 2 mm [pm^2cm^2/V^2]
CdTe	81.8	(2.81)	3.24	4.8	11.0
GaAs	65.6	4.18 (3.56)	3.59	0.5	4.21
GaP	24.8	3.67 (3.16)	3.34	0.2	0.72
ZnTe	68.5	3.13 (2.81)	3.17	1.3	7.27
GaSe	28.0	3.13 (2.82)	3.27	0.5	1.18
$sLiNbO_3$ @ 300 K @ 100 K	168	2.25 (2.18)	4.96	17 4.8	18.2 48.6

Nonlinear optical materials for THz generation

For common $LiNbO_3$, $v_g > v(\Omega)$, phase-mismatching

- Cherenkov radiation
- Low efficiency
- Not plane wave → Bad for applications

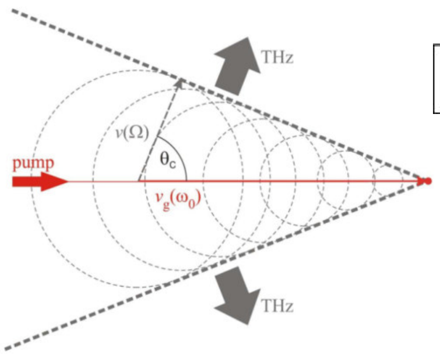

Tilted Pulse Front in LiNbO3

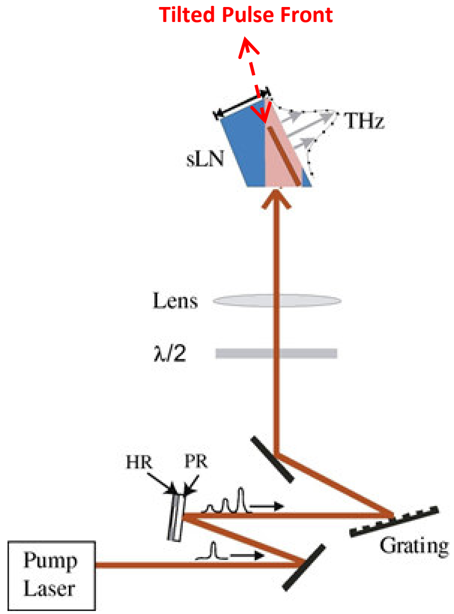

Prof. Dr. János Hebling
Department of Experimental Physics,
University of Pécs

Phonon-polariton dispersion of LN

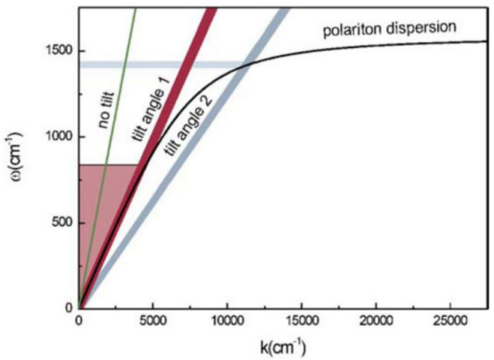

For ~ mJ, ~ 100 fs, 800 nm pulses,→~ uJ, ~100 kV/cm THz E-field.

K.L. Yeh *et al*, Opt. Comms. **281**, 3567 (2008).

Table-top, Laser-based, Intense THz source: organic crystals

PNPA, DAST & OH1: ~ 1200 to 1550 nm

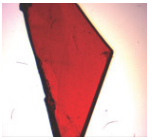

PNPA

PNPA
Pumping wavelengths ~ 1200 2100 nm, optimal wavelength of 1550 nm.

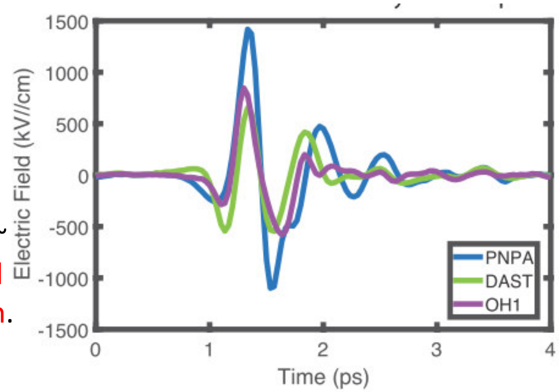

DAST

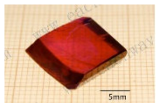

OH1

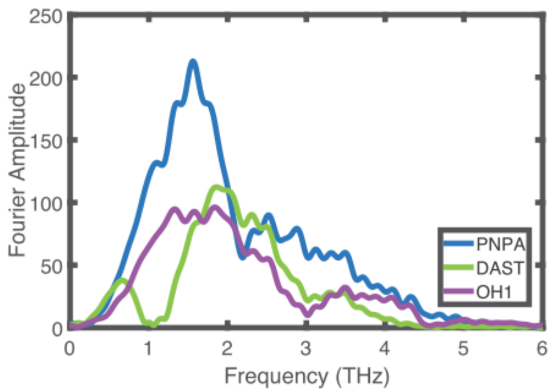

http://www.eachwave.com/Product/7304151453.html

BNA: ~ 800 nm

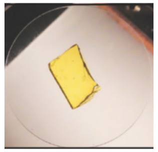

BNA

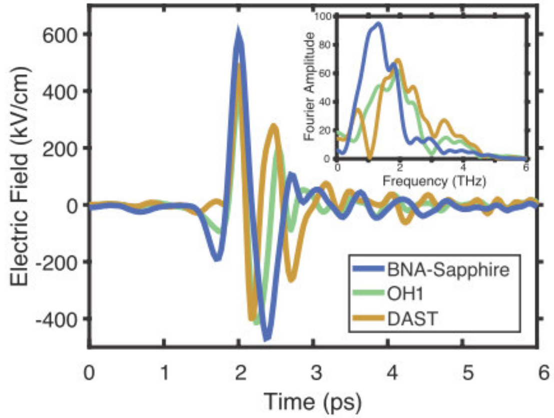

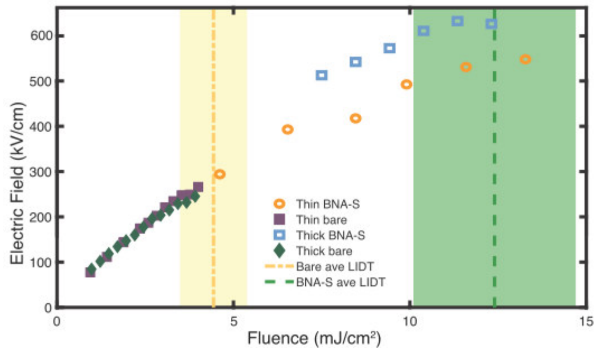

https://www.terahertzinnovations.com/

Linear vs. Nonlinear THz spectroscopy

- **Linear THz spectroscopy**
  $E_{max} \approx 100$ V/cm, pJ pulse energy
  THz probe, THz Time domain Spectroscopy of materials.

- **Nonlinear THz spectroscopy**
  $E_{max} \approx 100$ kV/cm, μJ pulse energy
  THz pump—THz / optical / X-ray / etc. probe measurements of dynamics

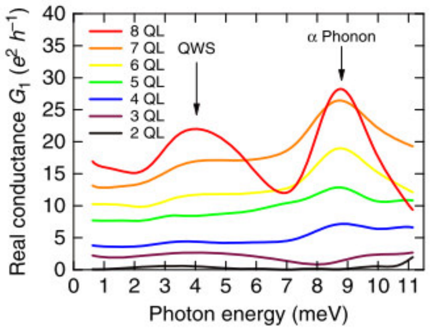

Conductance of TIs thin film by THz TDS.

For a 1 μJ, half-cycle THz pulse, focused into a volume of 1 mm^3 or less.

- E-field = $[2D_E/\varepsilon_0]^{1/2}$ ~ 100 kV/cm.
  → Use large electric field to displace atoms in polar solids
  (structural phase transitions, soft modes, …)

- H-field = E/c ~ 0.03 T
  → Use transient magnetic field to create magnetic/spin excitations

Intense THz applications: Scientific cases

Controlling lattice vibrations:

Intense THz **E-field** drive the phonon soft-mode of $SrTiO_3$

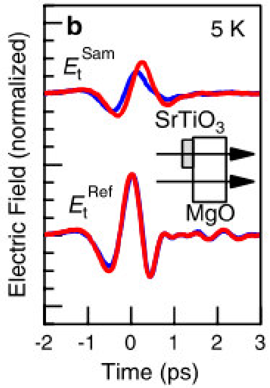

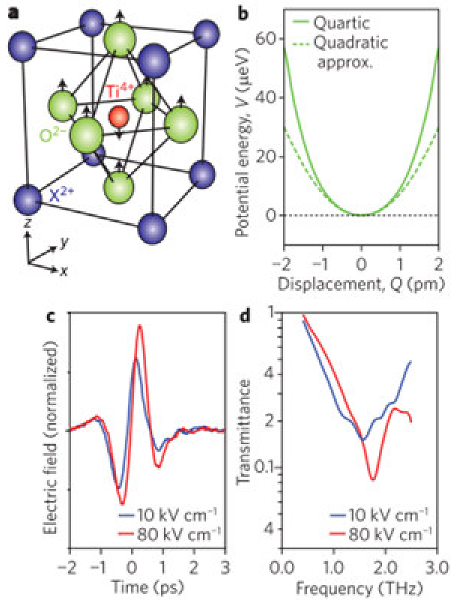

- The unit cell of $SrTiO_3$ and the arrows represent the direction of the soft-mode motion pf optical phonon.
- THz transmittance spectrum of a $SrTiO_3$ thin film shows a blue-shit of the resonance frequency and it indicates the soft-mode becomes stiffer/harder.

I. Katayama *et al*, PRL **108**, 907401 (2012).

Spin wave control in antiferromagnets:

Intense THz **B-field** excited the magnon mode of NiO.

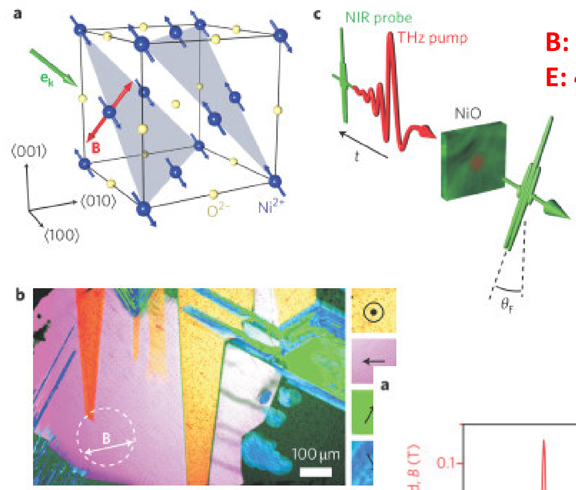

B: ~ 0.13 T
E: 400 kV/cm

An Intense THz pulse excites magnon coherently in NiO, and a following near-infrared pulse probes the magnetic dynamics by the mean of Faraday effect.

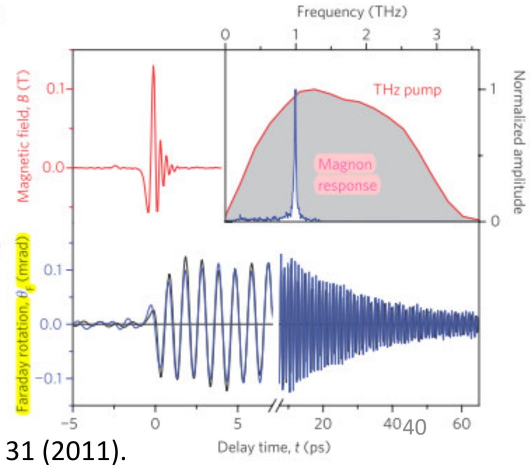

T. Kampfrath *et al*, Nat. Photon. **5**, 31 (2011).

Intense THz applications: THz E-field driven Phonon upconversion

Nonlinear Phonon response: Intense THz **E-field** driven the **phonon upconversion** of $SrTiO_3$

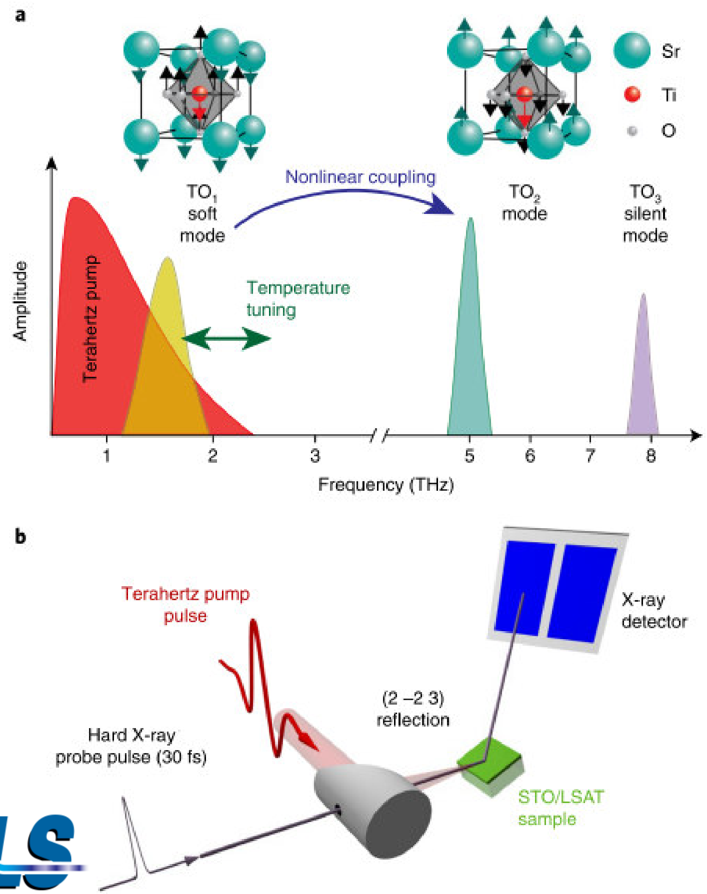

E^{THz}~880 kV/cm

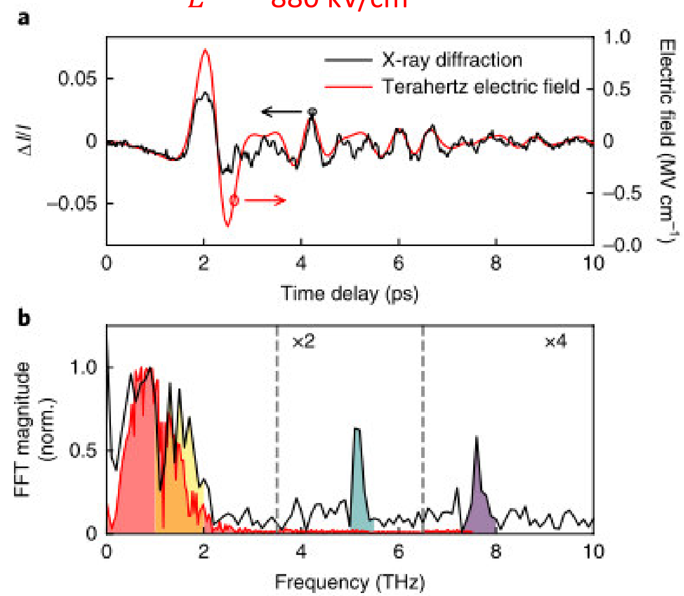

- XRD time-domain traces follow the THz E-field waveforms
- Higher frequencies of phonon modes are observed.
  → Phonon upconversion

M. Kozina *et al*, Nat. Phys. **15**, 387 (2019).

Intense THz Time-resolved ARPES: TI Bi_2Te_3

LETTER

https://doi.org/10.1038/s41586-018-0544-x

Subcycle observation of lightwave-driven Dirac currents in a topological surface band

J. Reimann[1], S. Schlauderer[2], C. P. Schmid[2], F. Langer[2], S. Baierl[2], K. A. Kokh[3,4], O. E. Tereshchenko[4,5], A. Kimura[6], C. Lange[2], J. Güdde[1], U. Höfer[1]* & R. Huber[2]*

Reg Amp: λc = 807 nm, 5.5 mJ, 33 fs @ 3 kHz

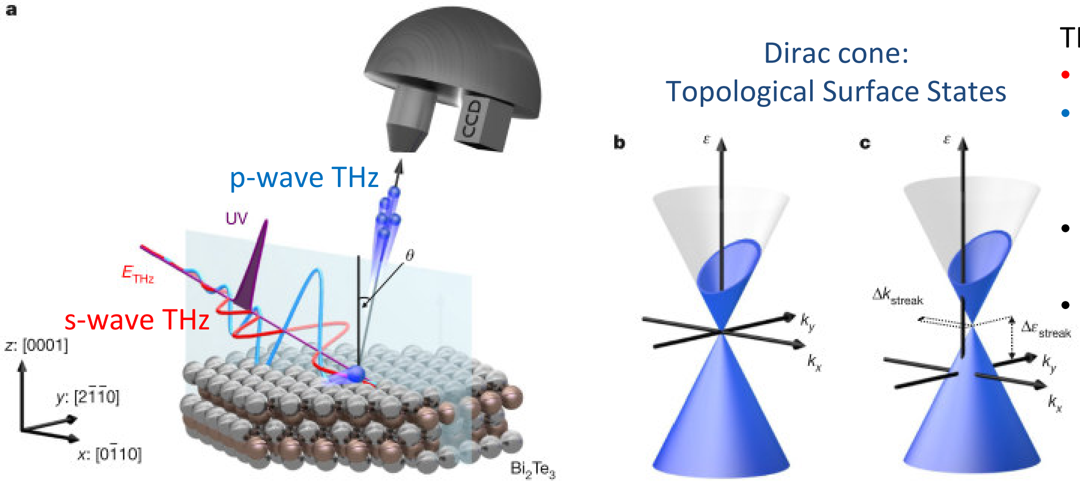

THz excitation:

- **s-wave**: Fermi surface shift, accelerating Dirac Fermion
- **p-wave** → energy shift $\Delta\varepsilon_{streak}$
  and/or momentum shift Δk_{streak}

- THz “carrier-wave” driven Dirac current: ballistic transport
- 1st observation of electron current driven by EM carrier wave.

J. Reimann *et al*, Nature **562**, 396 (2018)

THz Time-resolved ARPES spectra of TI Bi_2Te_3: **s-polarized** THz excitation

T = 80 K

Spectrum integration

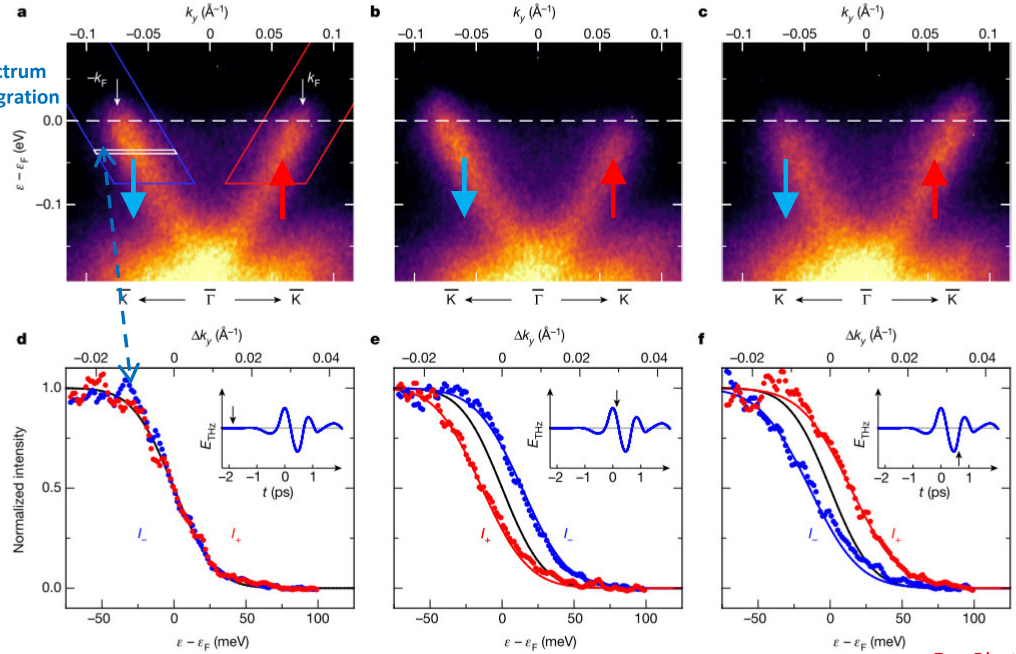

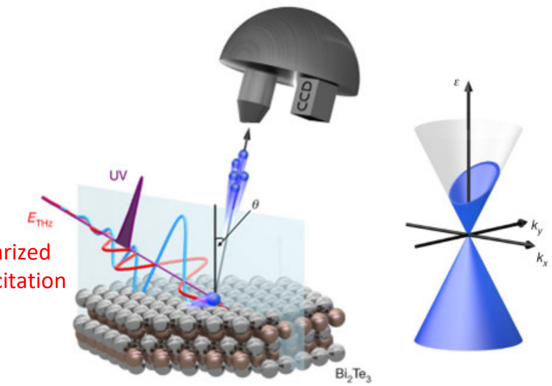

s-polarized THz excitation

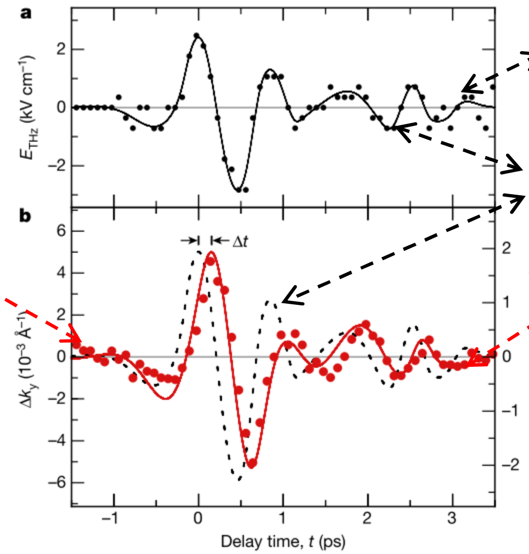

Reconstructed THz E-field

Spline

Exp Photoemission intensity

Simulated current density

s-polarized THz excitation:

- Asymmetric population of TSSs
- TSSs momentum shift COHERENTLY driven by THz "carrier-wave"
  → Dirac current: Ballistic transport
  Fermi velocity = 410 nm/ps, mean free path = 137 nm >> FinFET gate ~ 10 nm
- 1st observation of electron current driven by EM carrier wave in solid.

Accelerator-based Intense THz sources

Coherent Transition Radiation: CTR

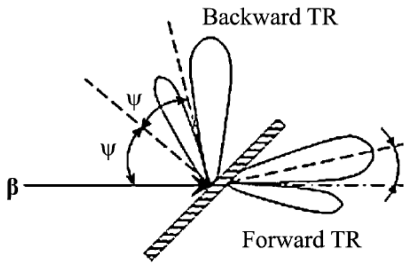

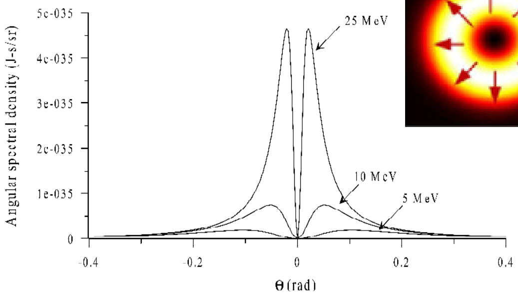

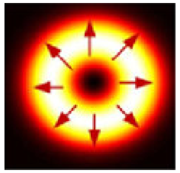

Spectral angular distribution of the emitted TR

$$\frac{dW}{d\omega d\Omega} = \frac{e^2\beta^2 \sin^2\theta}{\pi^2 c(1-\beta^2 \sin^2\theta)^2}$$

θ is the emission angle with respect to the electron beam axis.

- Transition radiation (TR) is emitted when a charged particle passes through the boundary of two media with different dielectric constant. Forward TR and backward TR occur simultaneously.
- The radiation intensity increases from zero in the forward direction to a broad peak at an angle $\theta \sim {}^{1}/_{\gamma}$.

Coherent Undulator Radiation : CUR

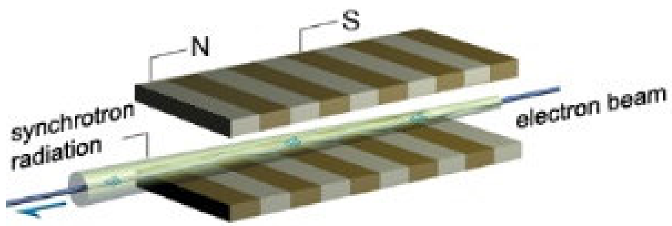

Radiation wavelength

$$\lambda = \frac{\lambda_u}{2\gamma^2}\left(1 + \frac{K^2}{2} + \gamma^2\theta^2\right)$$

λ_u: undulator period

K: undulator strength

$K = 0.9337\hat{B}\ [T]\ \lambda_u\ [cm]$

Ref: C.S. Thongbai and T. Vilaithong, Nucl. Instr. And Meth. A. 581 (2007) 874

Intense CTR THz source @ SPARC_Lab

SPARC_Lab:
Coherent Transition Radiation THz source
E_{THz} > 1 $MVcm^{-1}$, 0.5 - 5 THz @ ~ 10 Hz

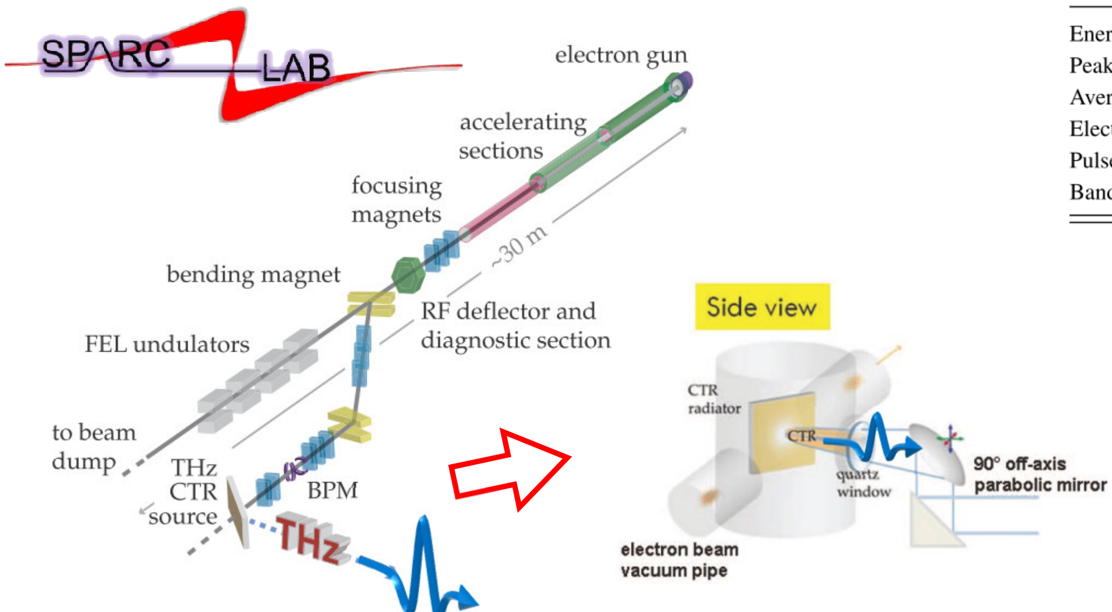

FIG. 1. SPARC schematic layout with the THz source placed at the end of the by-pass line.

TABLE I. SPARC-LAB THz source performance: radiation parameters.

	Single bunch	Four-bunches per train
Energy per pulse (μJ)	>1	0.6 @ 1 THz
Peak power (MW)	100	3 @ 1 THz
Average power (W)	1.8 10^{-4}	6 10^{-6}
Electric field (kV/cm)	>100	>10
Pulse duration (fs)	<200	<100
Bandwidth (%)	…	<25

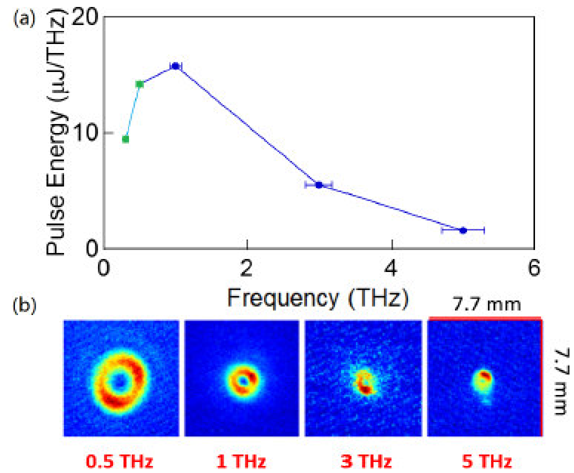

https://sparclab.lnf.infn.it/sparc_lab-home/sparc-linac/thz-source-and-experiments/

THz Third Harmonic Generation-TI Bi_2Se_3

Intense CTR THz source (Broadband)

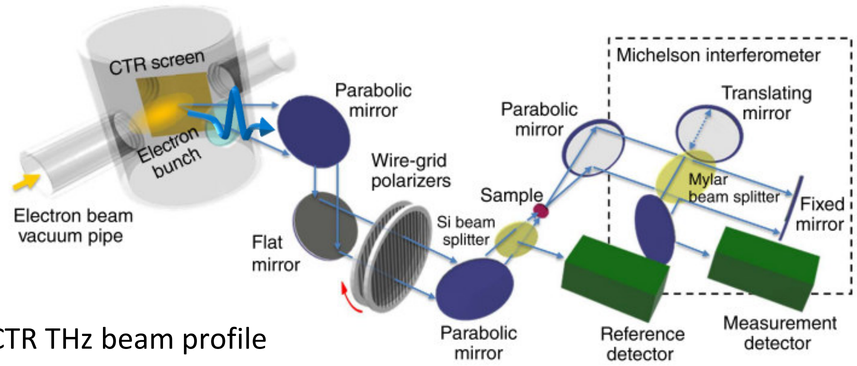

CTR THz beam profile

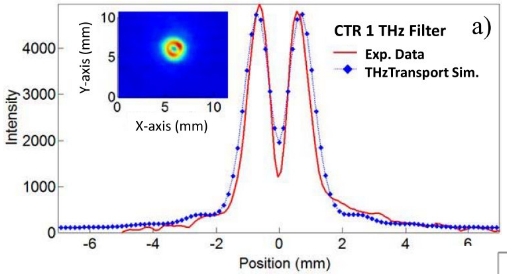

CTR THz spectrum

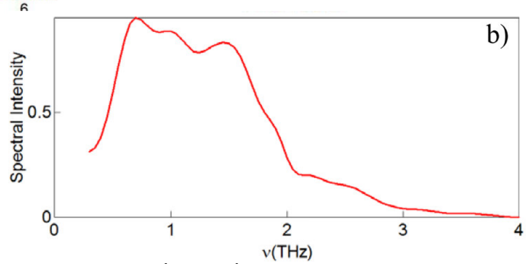

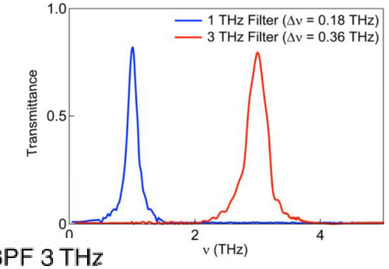

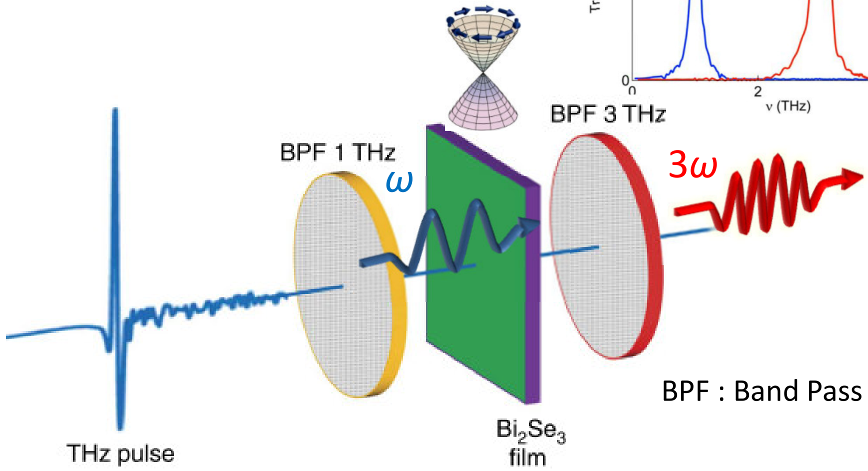

BPF : Band Pass Filter

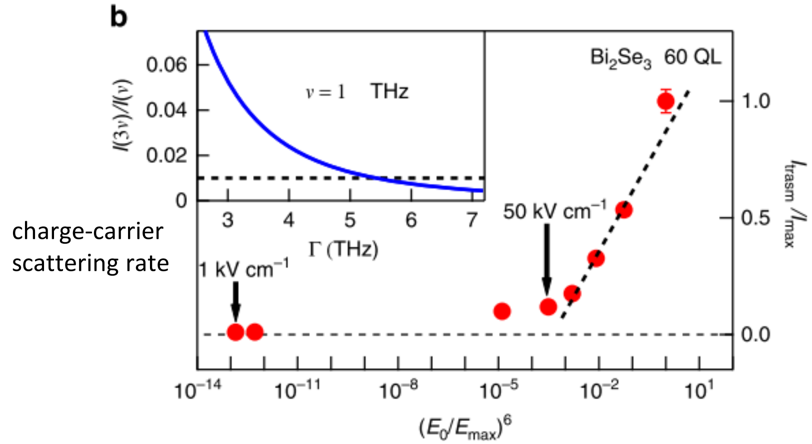

F. Giorgianniv et al,. Nat. Commun. **7**, 11421 (2016)

NarrowBand THz source @ HZDR

TELBE :
Superconducting RF accelerator-based superradiant THz source
E_{THz} = 12-85 kVcm^{-1}, 0.1-1.2 THz @ ~ 100 kHz

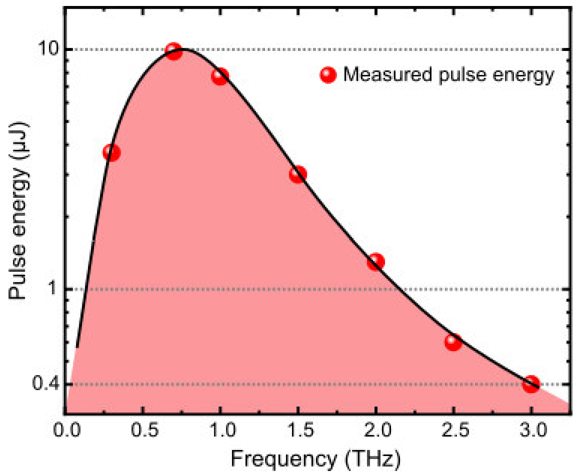

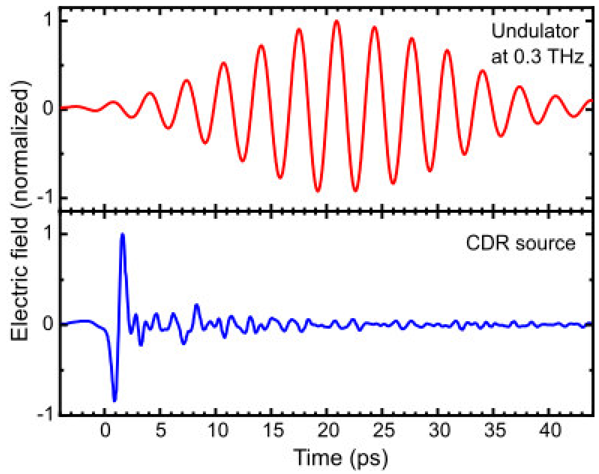

HELMHOLTZ ZENTRUM DRESDEN ROSSENDORF

NarrowBand THz High Harmonic Generation-Graphene

Graphene: Nonlinear THz Generation

Time-dependent conductivity
ΔQ : heat accumulation

$\sigma(\Delta Q, t)$

$j(t) = \sigma(\Delta Q, t)E_f(t)$
Temporal current modulation
Nonlinear current

$E_{HHG}^{THz}\ (t)$

THz emission

Ohm's law

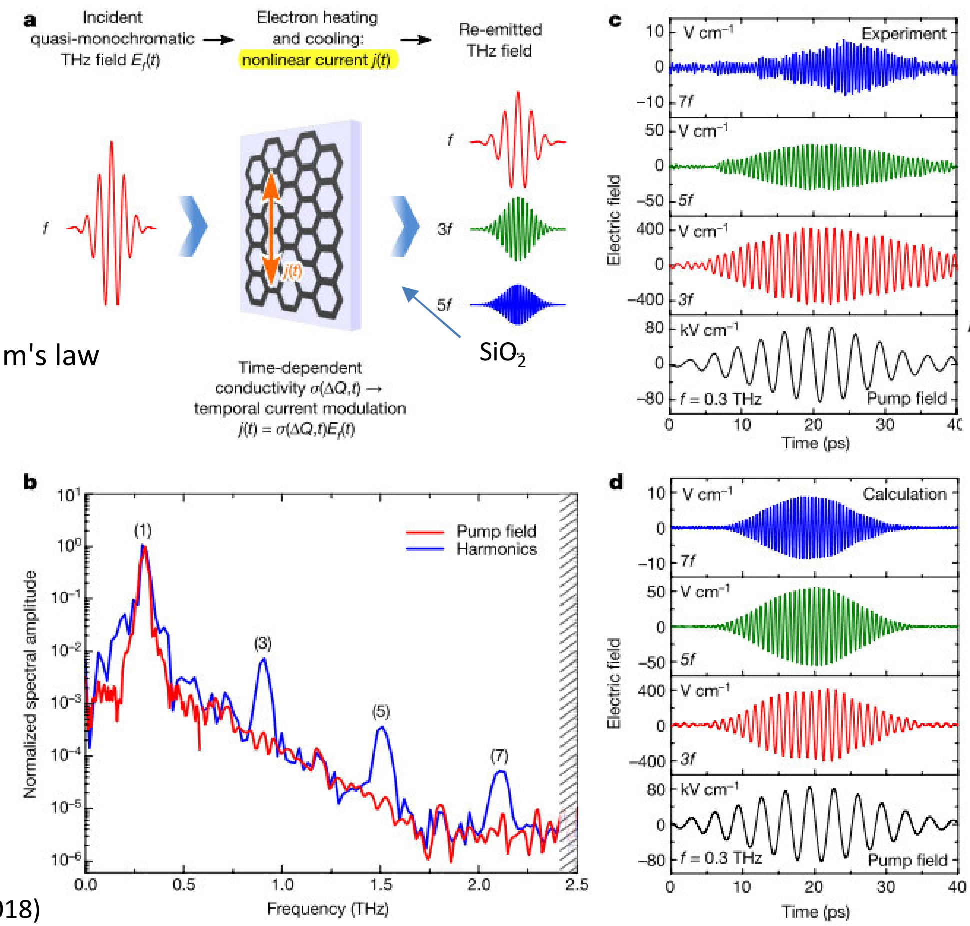

H. A. Hafez et al,. Nature. **561**, 507 (2018)

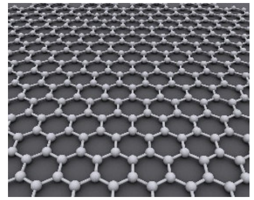

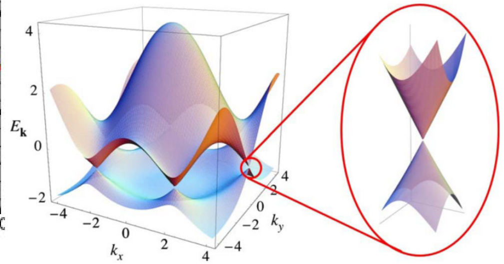

A. H. Castro Neto et al,.
Rev. Mod. Phys. **81**, 109 (2009)

Conversion efficiency

$$\frac{E_{3f}}{E_{1f}} : \frac{E_{5f}}{E_{1f}} : \frac{E_{7f}}{E_{1f}} = 10^{-3} : 10^{-4} : 10^{-5}$$

NarrowBand THz High Harmonic Generation-Graphene

Graphene: Nonlinear THz Generation

Time-dependent conductivity
ΔQ : heat accumulation

$\sigma(\Delta Q, t)$

$j(t) = \sigma(\Delta Q, t) E_f(t)$
Temporal current modulation
Nonlinear current

$E_{HHG}^{THz}\ (t)$

THz emission

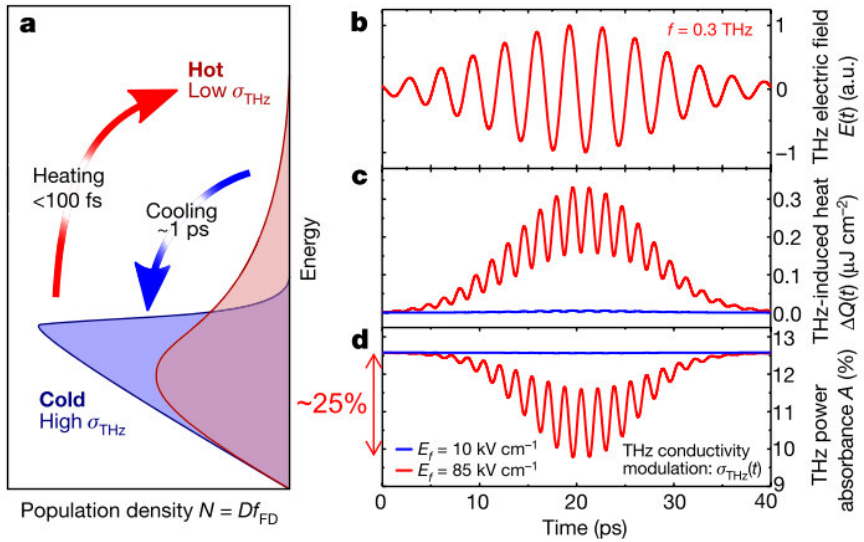

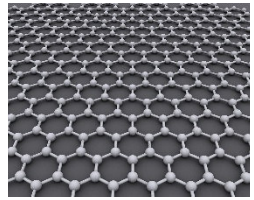

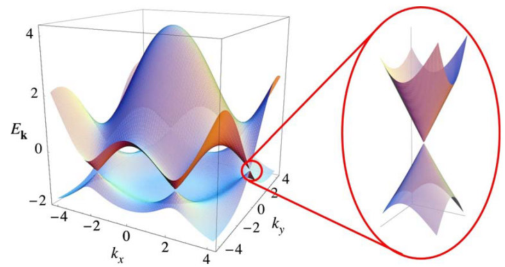

A. H. Castro Neto et al,.
Rev. Mod. Phys. **81**, 109 (2009)

H. A. Hafez et al,. Nature. **561**, 507 (2018)

NarrowBand THz HHG-Topological Materials

Topological Insulators: Bi_2Te_3

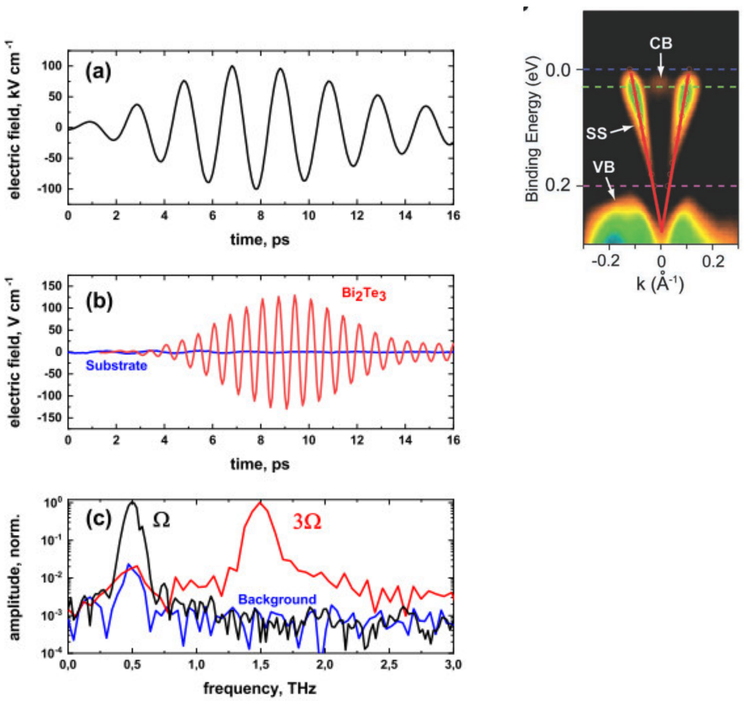

THz third-harmonic generation in Bi_2Te_3

S. Kovalev, et al. npj Quantum Materials **6**, 84 (2021)

Dirac Semimetal: Cd_3As_2

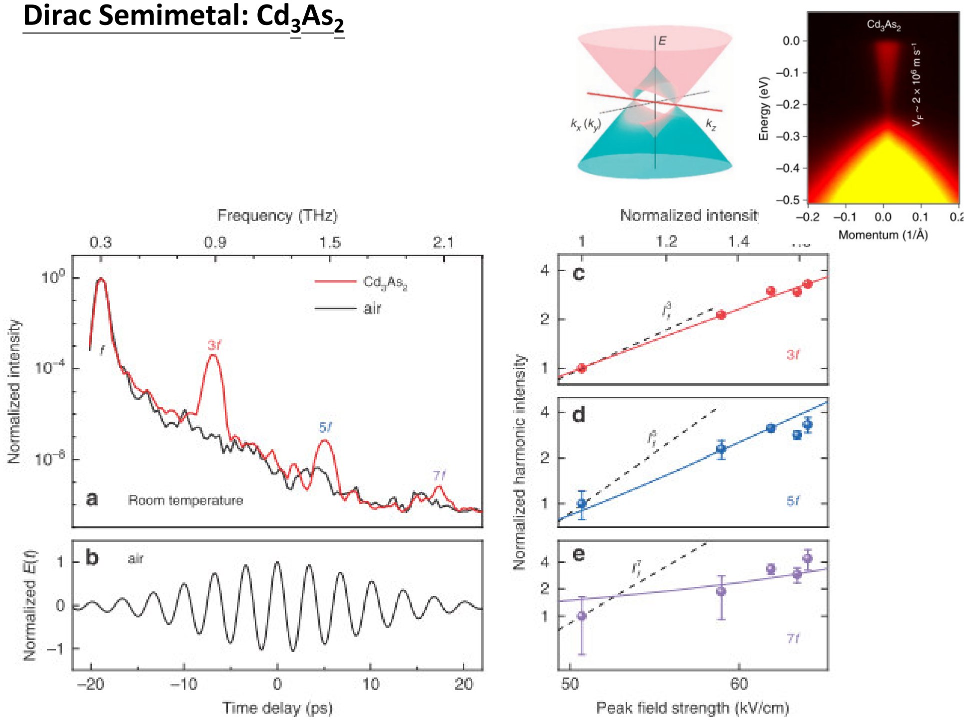

High-harmonic generations in Cd_3As_2

S. Kovalev, et al,. Nat. Commun. **11**, 2451 (2020)

NarrowBand THz HHG-Topological Materials

Topological Insulators: Bi_2Te_3

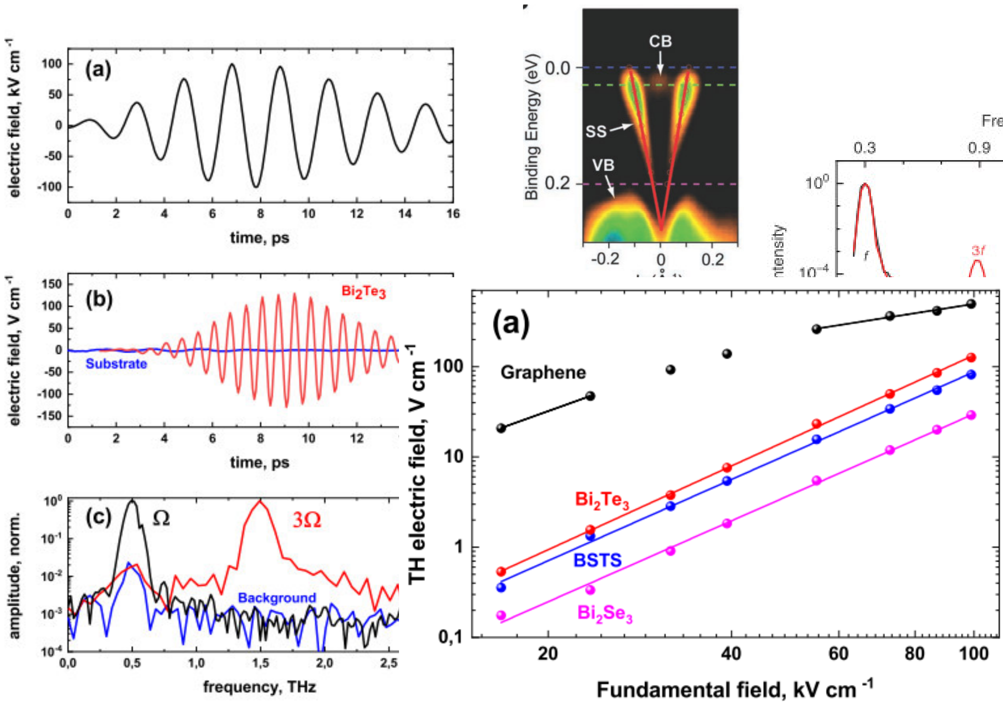

THz third-harmonic generation in Bi_2Te_3

S. Kovalev, et al. npj Quantum Materials **6**, 84 (2021)

Dirac Semimetal: Cd_3As_2

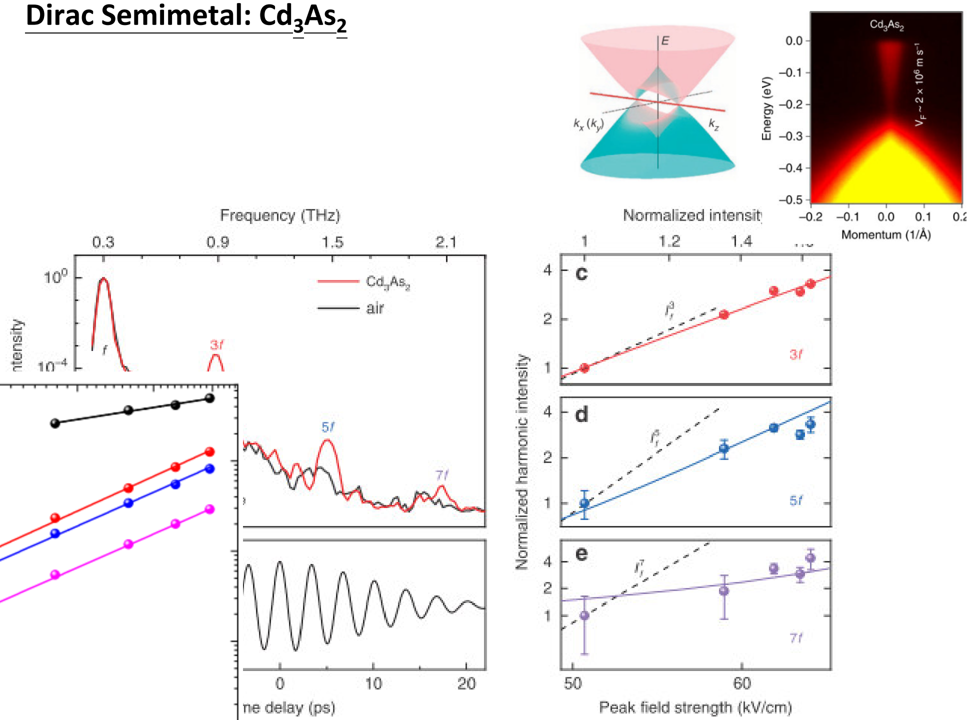

High-harmonic generations in Cd_3As_2

S. Kovalev, et al,. Nat. Commun. **11**, 2451 (2020)

Coherent THz Sources at NSRRC

THz Signal vs. Electron Number

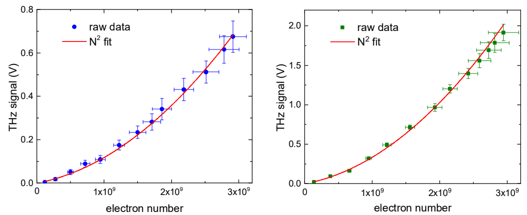

Bunch length measurement

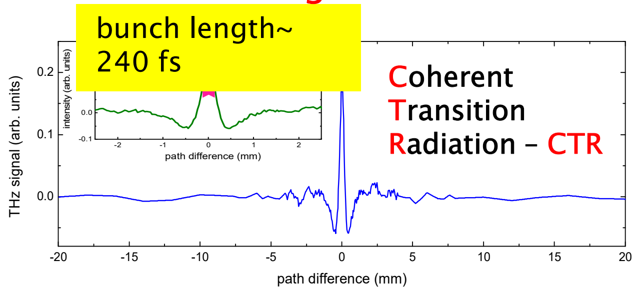

Superradiant THz FEL spectru

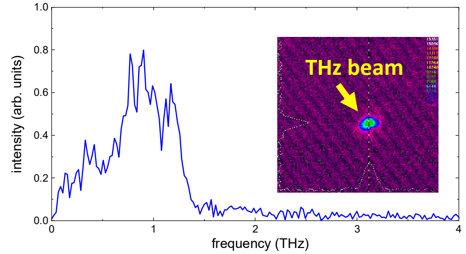

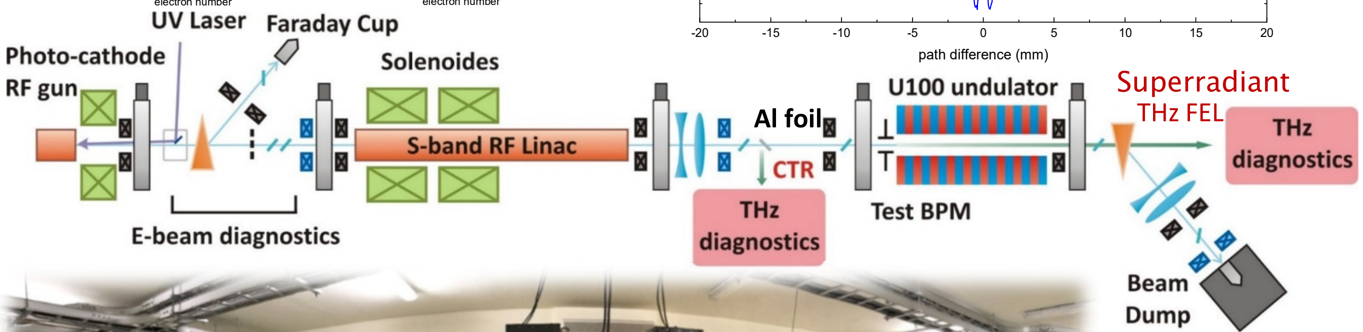

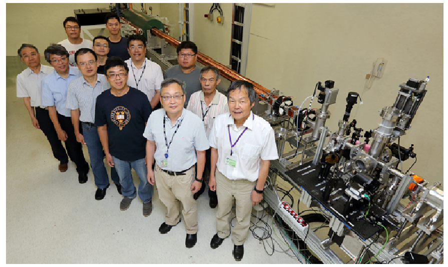

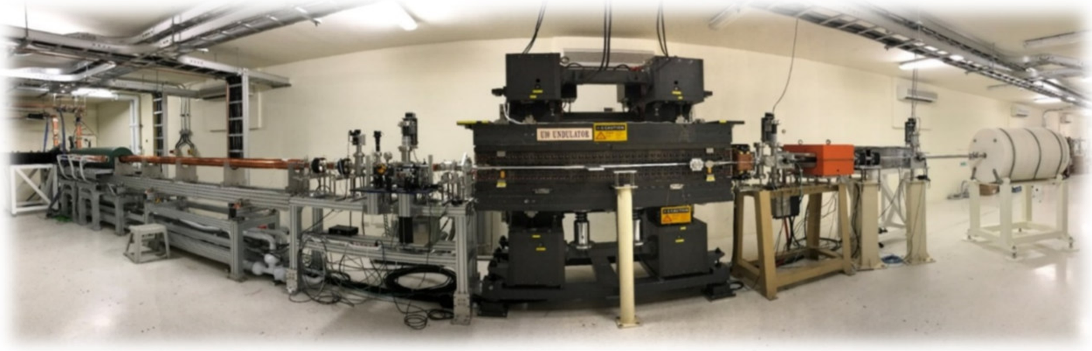

THz Parameters	CTR	Superradiant FEL
frequency (THz)	--	0.6 ~ 1.4
bandwidth	--	15%
energy (μJ)	2	20
Pulse duration	300 fs	18 ps
Peak power (MW)	6.6	1.1
Peak field (kV/cm)	400	163

Accelerator-based intense THz source@NSRRC

Photoinjector and coherent THz radiation sources

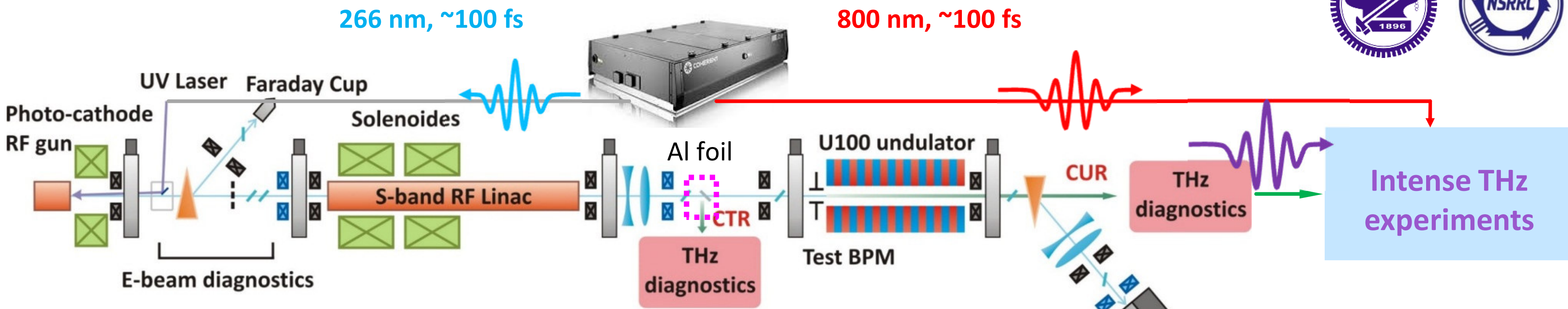

The 1st image of beam profile of intense THz radiation from an accelerator in Taiwan

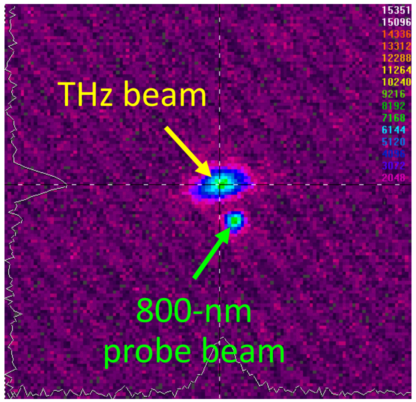

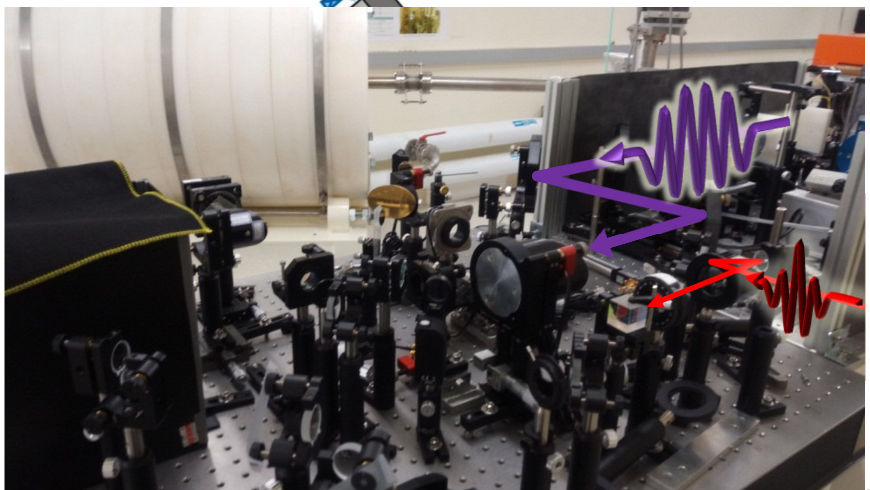

Thank you for your attention!